

**Deanship of Graduate Studies
Al-Quds University**



**Synthesis and Activation of Bitter Taste Receptor 14 (TAS2R14)
Agonists – An Approach for Assigning Its Active Site**

Hothyfah Rushdi Kittaneh

M.Sc. Thesis

Jerusalem-Palestine

1438 / 2017

**Synthesis and Activation of Bitter Taste Receptor 14 (TAS2R14) Agonists – An Approach
for Assigning Its Active Site**

Prepared By:

Hothyfah Rushdi Kittaneh

B.Sc., Pharmacy, Al-Quds University, Palestine.

Supervisor

Prof. Dr. Rafik Karaman

A thesis submitted in partial fulfillment of requirements for the degree of Master of Pharmaceutical Industry in Applied and Industrial Technology, Al-Quds University.

1438/2017

Al-Quds University
Deanship of Graduate Studies
Pharmaceutical Science Program



Thesis Approval

**Synthesis and Activation of Bitter Taste Receptor 14 (TAS2R14) Agonists – An Approach
for Assigning Its Active Site**

Prepared by: Hothyfah Rushdi Kittaneh

Registration No.: 20920189

Supervisor: Prof. Dr. Rafik Karaman

Master thesis Submitted and Accepted, Date:

The names and signatures of the examining committee members are as follows:

1- Head of Committee: Prof. Dr. Rafik Karaman

Signature:

2- Internal Examiner: Dr.

Signature:

3- External Examiner:

Signature:

Jerusalem–Palestine

1438/2017

Dedication

This thesis is dedicated to my wonderful parents who sacrificed a lot for me to be what I am now.

I am very grateful for their unconditional love, support and prayers.

Thank you for instilling in me the desire to strive for the best.

I dedicate this thesis to my dear country, Palestine. My dear land that I believe

Strongly will return to us some day.

Hothyfah Kittaneh

Declaration

I certify that the thesis submitted for the degree of master is the result of my own research, except where otherwise acknowledged, and that this thesis (or any part of the same) has not be submitted for a higher degree to any other university or institution.

Signed: 

Hothyfah Rushdi Kittaneh

Date:

Acknowledgment

First and foremost, I am deeply thankful to Almighty **Allah** from whom I always receive help and protection.

I would like to express my special appreciation and thanks to my supervisor Professor Dr. Rafik Karaman, I would like to thank you for encouraging my research and for allowing me to grow as a researcher.

A very special thanks to my father Dr. Rushdi Kittaneh, who has encouraged, supported me through the dark times, celebrated with me through the good, who has been an excellent teacher.

A special thanks to my family. Words cannot express how grateful I am to my mother, for all of the sacrifices that you've made. Your prayer for me was what sustained me thus far. I would also like to thank all of my friends who supported me in writing and gave me the incentive to strive towards my goal.

Abstract

Sensing potentially harmful bitter substances in the oral cavity is achieved by a group of ~25 receptors, named TAS2Rs, which are expressed in specialized sensory cells and recognize individual but overlapping sets of bitter compounds. The receptors differ in their tuning breadths ranging from narrowly to broadly tuned receptors. One of the most broadly tuned human bitter taste receptors is the TAS2R14 recognizing an enormous variety of chemically diverse synthetic and natural bitter compounds, including numerous medicinal drugs. This suggests that this receptor possesses a large readily accessible ligand binding pocket. To allow probing the accessibility and size of the ligand binding pocket. Mefenamic acid (2-(2,3-dimethylphenyl)aminobenzoic acid) and diclofenac (2-(2,6-dichloranilino) phenylacetic acid) have been identified as novel TAS2R14 agonists in a recent *in silico* screening of agonists and confirmed by functional assays, a previously identified TAS2R14 agonist. Benzoin (2-hydroxy-1,2-di(phenyl)ethanone), which represents the most simple aromatic hydroxyl ketone and is a naturally in bitter almond oil, also belongs to TAS2R14 agonists. Bad contacts were observed between the hydrogen of the ligand alkoxy groups and the backbone I1262^{7,35}, diclofenac derivatives cannot be accommodated in the binding pocket because of steric hindrance. The resulting mefenamic acid benzyl ester retained agonistic properties, although the lack of receptor activation below a concentration of 10 μ M indicates reduced potency. For both benzoin derivatives receptor responses already at concentrations of 10 μ M, whereas the necessary concentration of unmodified benzoin required to activate TAS2R14 was ~10-fold higher. Mefenamic acid and diclofenac show an intramolecular H-bond between the alkoxy group and the aniline nitrogen, not present in the benzoin structure. Different derivatives alkyl/ benzyl of diclofenac, mefenamic acid and benzoin were synthesized and tested against TAS2R14. The derivatives with global minima with the substituent positioned far from the core of the compound skeleton structure (aniline nitrogen or carbonyl group), such as mefenamic acid hexyl, mefenamic acid decyl esters, benzoin benzyl and benzoin hexyl ethers, cause the activation of TAS2R14 to a variable extent, while the compounds with global minima for which substituent is placed near the structural core of the compound, such as in diclofenac derivatives, did not activate TAS2R14. Therefore, the difference between the mefenamic acid and benzoin derivatives on the one hand and the diclofenac derivatives on the other hand can be attributed to steric effects.

Table of Contents

Declaration	I
Acknowledgments	II
Abstract	III
Table of Contents	IV
List of Tables	VI
List of Schemes	VI
List of Figures	VII
List of Abbreviations	IX
Introduction	
1. Introduction.....	2
1.1 Background:	2
1.1.1 Taste Masking	4
1.1.2 Challenges and Criteria for Pursuing Masking Bitter Taste Approaches	4
1.2 Bitter Taste Masking Approaches (Techniques).....	5
1.3 Human Bitter Taste Receptors	9
1.4 General Objective	Error! Bookmark not defined.1
Literature Review	
2. Literature Review	Error! Bookmark not defined.3
2.1 Bitter Taste Masking	Error! Bookmark not defined.3
2.2 Selected Drugs	Error! Bookmark not defined.4
2.2.1 Mefenamic Acid:	Error! Bookmark not defined.4
2.2.2 Diclofenac.....	15
Expierimental	
3. Materials and Methods.....	Error! Bookmark not defined.17
3.1 Chemical Syntheses and Analysis.....	Error! Bookmark not defined.17

3.2 Synthesis of Bitter Taste Derivatives.....	18
3.2.1 Preparation of Mefenamic Acid, and Diclofenac Alkyl Esters	18
3.2.2 Preparation of Benzoin Alkyl Ethers	Error! Bookmark not defined.1
3.3 Functional Calcium Imaging Experiments.....	Error! Bookmark not defined.2
3.4 Computational Analysis	Error! Bookmark not defined.2
3.5 Homology Modeling.....	Error! Bookmark not defined.3
3.6 Docking	Error! Bookmark not defined.3
Results and Discussion	
4. Results and Discussion.....	Error! Bookmark not defined.6
4.1 Synthesis Characterization.....	26
4.2 Discussion.....	Error! Bookmark not defined.7
4.3 Summary52
References:.....	Error! Bookmark not defined.53
ملخص.....	58

List of tables

Table no.	Title	Page
Table 1	Specific area of tongue.	10
Table 2	Glide XP scores for mefenamic acid, diclofenac, benzoin and their derivatives in complex with TAS2R14 structure.	52

List of schemes

Scheme no.	Title	Page
Scheme 1	Synthesis of mefenamic hexyl (S9)	18
Scheme 2	Synthesis of mefenamic acid with benzyl bromide (S10)	19
Scheme 3	Synthesis of mefenamic decyl	19
Scheme 4	Synthesis of diclofenac benzyl	20
Scheme 5	Synthesis of diclofenac hexyl	20
Scheme 6	Synthesis of benzoin with benzyl bromide (S12)	21
Scheme 7	Synthesis of benzoin with iodohexane (S13)	22

List of figures

Figure no.	Title	Page
Figure 1	Locations of taste sensors on the tongue	10
Figure 2	¹ H-NMR spectrum of mefenamic acid in CD3OD S8	26
Figure 3	IR result of mefenamic acid	27
Figure 4	¹ H-NMR spectrum of mefenamic hexyl in CD3OD S9	27
Figure 5	IR spectrum of mefenamic hexyl S9	28
Figure 6	LC-MS spectrum for mefenamic hexyl ester	28
Figure 7	¹ H-NMR spectrum of mefenamic benzyl in CD3OD S10	29
Figure 8	IR spectrum of mefenamic benzyl	29
Figure 9	LC-MS spectrum mefenamic benzyl ester	30
Figure 10	¹ H-NMR spectrum of mefenamic decyl in CD3OD	30
Figure 11	IR spectrum of mefenamic decyl	31
Figure 12	IR spectrum of diclofenac	31
Figure 13	IR spectrum of diclofenac hexyl ester	32
Figure 14	¹ H-NMR spectrum of diclofenac hexyl ester in CD3OD	32
Figure 15	LC-MS spectrum of diclofenac hexyl ester	32
Figure 16	¹ H-NMR spectrum of diclofenac benzyl ester in CD3OD	33
Figure 17	IR spectrum of diclofenac benzyl ester	33
Figure 18	LC-MS spectrum of diclofenac benzyl ester	34
Figure 19	IR spectrum of benzoin	34
Figure 20	¹ H-NMR spectrum of benzoin hexyl in CDCl ₃	35
Figure 21	IR spectrum of benzoin hexyl	35
Figure 22	¹ H-NMR spectrum of benzoin benzyl in CDCl ₃	36
Figure 23	IR spectrum of benzoin benzyl	36
Figure 24	LC-MS spectrum for benzoin benzyl ether	36
Figure 25	Chemical structures of the cognate TAS2R14 agonists	43
Figure 26	Chemical structures, DFT-calculated 3D-cell volumes	44

Figure 27	Chemical structures, DFT-calculated 3D-cell volumes, and receptor activating properties of benzoin derivatives	45
Figure 28	Sequence alignment of modeled TAS2R14 receptor and the template X-ray structure of β 2 adrenergic receptor	46
Figure 29	3D and 2D representation of the docking pose of mefenamic acid (A), diclofenac (B), benzoin (C) and their derivatives	47
Figure 30	The mefenamic acid (S8) standard shows in the graph bitterness	49
Figure 31	For benzoin (S11) the bitterness	50

List of Abbreviations

Abbreviations	Definition
DFT	Density functional theory
DMF	Dimethylformamide
HPLC	High-performance liquid chromatography
IR	Infrared
IUD	Intrauterine devices
LC-MS	Liquid chromatography-Mass spectrometry
M.P	Melting point
<i>m/z</i>	Mass-to-Charge ratio
NMR	Nuclear magnetic resonance
NSAIDs	Non-steroidal anti-inflammatory drugs
Ppm	Part per million
SIF	Simulated intestinal fluid
$t_{1/2}$	Half life
THF	Tetrahydrofuran
TLC	Thin layer chromatography

Abbriveation	Definition
DAG	Di-acyl glycerol
DPCs	Drug-polymer complexes
EC	Ethylcellulose
GPCRs	G-protein coupled receptors
HCl	Hydrochloride
KBr	Potassium bromide
MgSO4	Magnesium sulfide
NaOH	Sodium hydroxide
OTC	Over the counter
OTD	Orally-disintegrating tablet
PIP	Phosphatidylinositol-4,5-bisphosphate
PLC	Phospholipase C
PRCG	Polak-Ribiere Conjugate Gradient
RDT	Rapid disintegrating tablet
SGF	Simulated gastric fluid
SSF	Simulated salivary fluid
TAS2R	Taste receptor type2
TRPM5	Transient receptor potential channel
XP	Extra Precision

Acknowledgment

First and foremost, I am deeply thankful to Almighty **Allah** from whom I always receive help and protection.

I would like to express my special appreciation and thanks to my supervisor Professor Dr. Rafik Karaman, I would like to thank you for encouraging my research and for allowing me to grow as a researcher.

A very special thanks to my father Dr. Rushdi Kittaneh, who has encouraged, supported me through the dark times, celebrated with me through the good, who has been an excellent teacher.

A special thanks to my family. Words cannot express how grateful I am to my mother, for all of the sacrifices that you've made. Your prayer for me was what sustained me thus far. I would also like to thank all of my friends who supported me in writing and gave me the incentive to strive towards my goal.

Abstract

Sensing potentially harmful bitter substances in the oral cavity is achieved by a group of ~25 receptors, named TAS2Rs, which are expressed in specialized sensory cells and recognize individual but overlapping sets of bitter compounds. The receptors differ in their tuning breadths ranging from narrowly to broadly tuned receptors. One of the most broadly tuned human bitter taste receptors is the TAS2R14 recognizing an enormous variety of chemically diverse synthetic and natural bitter compounds, including numerous medicinal drugs. This suggests that this receptor possesses a large readily accessible ligand binding pocket. To allow probing the accessibility and size of the ligand binding pocket. Mefenamic acid (2-(2,3-dimethylphenyl)aminobenzoic acid) and diclofenac (2-(2,6-dichloranilino) phenylacetic acid) have been identified as novel TAS2R14 agonists in a recent *in silico* screening of agonists and confirmed by functional assays, a previously identified TAS2R14 agonist. Benzoin (2-hydroxy-1,2-di(phenyl)ethanone), which represents the most simple aromatic hydroxyl ketone and is a naturally in bitter almond oil, also belongs to TAS2R14 agonists. Bad contacts were observed between the hydrogen of the ligand alkoxy groups and the backbone I1262^{7,35}, diclofenac derivatives cannot be accommodated in the binding pocket because of steric hindrance. The resulting mefenamic acid benzyl ester retained agonistic properties, although the lack of receptor activation below a concentration of 10 μ M indicates reduced potency. For both benzoin derivatives receptor responses already at concentrations of 10 μ M, whereas the necessary concentration of unmodified benzoin required to activate TAS2R14 was ~10-fold higher. Mefenamic acid and diclofenac show an intramolecular H-bond between the alkoxy group and the aniline nitrogen, not present in the benzoin structure. Different derivatives alkyl/ benzyl of diclofenac, mefenamic acid and benzoin were synthesized and tested against TAS2R14. The derivatives with global minima with the substituent positioned far from the core of the compound skeleton structure (aniline nitrogen or carbonyl group), such as mefenamic acid hexyl, mefenamic acid decyl esters, benzoin benzyl and benzoin hexyl ethers, cause the activation of TAS2R14 to a variable extent, while the compounds with global minima for which substituent is placed near the structural core of the compound, such as in diclofenac derivatives, did not activate TAS2R14. Therefore, the difference between the mefenamic acid and benzoin derivatives on the one hand and the diclofenac derivatives on the other hand can be attributed to steric effects.

Table of Contents

Declaration	I
Acknowledgments	II
Abstract	III
Table of Contents	IV
List of Tables	VI
List of Schemes	VI
List of Figures	VII
List of Abbreviations	IX
Introduction	
1. Introduction.....	2
1.1 Background:	2
1.1.1 Taste Masking	4
1.1.2 Challenges and Criteria for Pursuing Masking Bitter Taste Approaches	4
1.2 Bitter Taste Masking Approaches (Techniques).....	5
1.3 Human Bitter Taste Receptors	9
1.4 General Objective	Error! Bookmark not defined.1
Literature Review	
2. Literature Review	Error! Bookmark not defined.3
2.1 Bitter Taste Masking	Error! Bookmark not defined.3
2.2 Selected Drugs	Error! Bookmark not defined.4
2.2.1 Mefenamic Acid:	Error! Bookmark not defined.4
2.2.2 Diclofenac.....	15
Expierimental	
3. Materials and Methods.....	Error! Bookmark not defined.17
3.1 Chemical Syntheses and Analysis.....	Error! Bookmark not defined.17

3.2 Synthesis of Bitter Taste Derivatives.....	18
3.2.1 Preparation of Mefenamic Acid, and Diclofenac Alkyl Esters	18
3.2.2 Preparation of Benzoin Alkyl Ethers	Error! Bookmark not defined.1
3.3 Functional Calcium Imaging Experiments.....	Error! Bookmark not defined.2
3.4 Computational Analysis	Error! Bookmark not defined.2
3.5 Homology Modeling.....	Error! Bookmark not defined.3
3.6 Docking	Error! Bookmark not defined.3
Results and Discussion	
4. Results and Discussion.....	Error! Bookmark not defined.6
4.1 Synthesis Characterization.....	26
4.2 Discussion.....	Error! Bookmark not defined.7
4.3 Summary52
References:.....	Error! Bookmark not defined.53
ملخص.....	58

List of tables

Table no.	Title	Page
Table 1	Specific area of tongue.	10
Table 2	Glide XP scores for mefenamic acid, diclofenac, benzoin and their derivatives in complex with TAS2R14 structure.	52

List of schemes

Scheme no.	Title	Page
Scheme 1	Synthesis of mefenamic hexyl (S9)	18
Scheme 2	Synthesis of mefenamic acid with benzyl bromide (S10)	19
Scheme 3	Synthesis of mefenamic decyl	19
Scheme 4	Synthesis of diclofenac benzyl	20
Scheme 5	Synthesis of diclofenac hexyl	20
Scheme 6	Synthesis of benzoin with benzyl bromide (S12)	21
Scheme 7	Synthesis of benzoin with iodohexane (S13)	22

List of figures

Figure no.	Title	Page
Figure 1	Locations of taste sensors on the tongue	10
Figure 2	¹ H-NMR spectrum of mefenamic acid in CD3OD S8	26
Figure 3	IR result of mefenamic acid	27
Figure 4	¹ H-NMR spectrum of mefenamic hexyl in CD3OD S9	27
Figure 5	IR spectrum of mefenamic hexyl S9	28
Figure 6	LC-MS spectrum for mefenamic hexyl ester	28
Figure 7	¹ H-NMR spectrum of mefenamic benzyl in CD3OD S10	29
Figure 8	IR spectrum of mefenamic benzyl	29
Figure 9	LC-MS spectrum mefenamic benzyl ester	30
Figure 10	¹ H-NMR spectrum of mefenamic decyl in CD3OD	30
Figure 11	IR spectrum of mefenamic decyl	31
Figure 12	IR spectrum of diclofenac	31
Figure 13	IR spectrum of diclofenac hexyl ester	32
Figure 14	¹ H-NMR spectrum of diclofenac hexyl ester in CD3OD	32
Figure 15	LC-MS spectrum of diclofenac hexyl ester	32
Figure 16	¹ H-NMR spectrum of diclofenac benzyl ester in CD3OD	33
Figure 17	IR spectrum of diclofenac benzyl ester	33
Figure 18	LC-MS spectrum of diclofenac benzyl ester	34
Figure 19	IR spectrum of benzoin	34
Figure 20	¹ H-NMR spectrum of benzoin hexyl in CDCl ₃	35
Figure 21	IR spectrum of benzoin hexyl	35
Figure 22	¹ H-NMR spectrum of benzoin benzyl in CDCl ₃	36
Figure 23	IR spectrum of benzoin benzyl	36
Figure 24	LC-MS spectrum for benzoin benzyl ether	36
Figure 25	Chemical structures of the cognate TAS2R14 agonists	43
Figure 26	Chemical structures, DFT-calculated 3D-cell volumes	44

Figure 27	Chemical structures, DFT-calculated 3D-cell volumes, and receptor activating properties of benzoin derivatives	45
Figure 28	Sequence alignment of modeled TAS2R14 receptor and the template X-ray structure of β 2 adrenergic receptor	46
Figure 29	3D and 2D representation of the docking pose of mefenamic acid (A), diclofenac (B), benzoin (C) and their derivatives	47
Figure 30	The mefenamic acid (S8) standard shows in the graph bitterness	49
Figure 31	For benzoin (S11) the bitterness	50

List of Abbreviations

Abbreviations	Definition
DFT	Density functional theory
DMF	Dimethylformamide
HPLC	High-performance liquid chromatography
IR	Infrared
IUD	Intrauterine devices
LC-MS	Liquid chromatography-Mass spectrometry
M.P	Melting point
<i>m/z</i>	Mass-to-Charge ratio
NMR	Nuclear magnetic resonance
NSAIDs	Non-steroidal anti-inflammatory drugs
Ppm	Part per million
SIF	Simulated intestinal fluid
$t_{1/2}$	Half life
THF	Tetrahydrofuran
TLC	Thin layer chromatography

Abbriveation	Definition
DAG	Di-acyl glycerol
DPCs	Drug-polymer complexes
EC	Ethylcellulose
GPCRs	G-protein coupled receptors
HCl	Hydrochloride
KBr	Potassium bromide
MgSO4	Magnesium sulfide
NaOH	Sodium hydroxide
OTC	Over the counter
OTD	Orally-disintegrating tablet
PIP	Phosphatidylinositol-4,5-bisphosphate
PLC	Phospholipase C
PRCG	Polak-Ribiere Conjugate Gradient
RDT	Rapid disintegrating tablet
SGF	Simulated gastric fluid
SSF	Simulated salivary fluid
TAS2R	Taste receptor type2
TRPM5	Transient receptor potential channel
XP	Extra Precision

Introduction

Chapter one

1. Introduction

1.1. Background:

The palatability of the active ingredient of a drug is a significant obstacle in developing a patient friendly dosage form. Organoleptic properties, such as taste, are an important factor when selecting a certain drug from the generic products available in the market that have the same active ingredient. It is a key issue for doctors and pharmacists administering the drugs and particularly for the pediatric and geriatric populations. Nowadays, pharmaceutical companies are recognizing the importance of taste masking and a significant number of techniques have been developed for concealing the objectionable taste [1].

The word “medicine” for a child is considered a bad thing to administer because of its aversive taste. Medicines dissolve in saliva and bind to taste receptors on the tongue giving a bitter, sweet, salty, sour, or umami sensation. Sweet and sour taste receptors are concentrated on the tip and lateral borders of the tongue respectively. Bitter taste is sensed by the receptors on the posterior part of the tongue and umami taste receptors are located all over the tongue. A short period after birth, infants reject bitter tastes and prefer sweet and umami tastes [1]. Children have larger number of taste buds than adults which are responsible for sensitivity toward taste. These taste buds regenerate every two weeks. Taste becomes altered as a function of the aging process, which explains why most children find certain flavors to be too strong when adults do not. The American Academy of Pediatrics estimates that compliance in children is as low as 53%, indicating that children frequently fail to take medications properly. Noncompliance can lead to: (1) persistent symptoms, (2) need for additional doctor visits or even hospitalizations, (3) worsening of condition, (4) need for additional medications, (5) increased healthcare costs and (6) development of drug-resistant organisms in cases of infectious diseases [2].

In mammals, taste buds are groups of 30-100 individual elongated "neuroepithelial" cells which are often embedded in special structure in the surrounding epithelium known as papillae. Just below the taste bud apex, taste cells are joined by tight junctional complexes that prevent gaps between cells. Food molecules cannot therefore squeeze between taste cells and get into the taste bud.

Taste papillae located on the tongue appear as little red dots, or raised bumps, particularly at the front of the tongue called "fungiform" papillae. There are three other kinds of papillae, foliate, circumvallate and the non-gustatory filiform. In mammals taste buds are located throughout the oral cavity, in the pharynx, the laryngeal epiglottis and at the entrance of the esophagus. Taste perception fades with age; on average, people lose half their taste receptors by time they turn 20 [3]. The sensation of taste can be categorized into five basic tastes: sweetness, sourness, saltiness, bitterness, and umami. Taste buds are able to differentiate among different tastes through detecting interaction with different molecules or ions. Sweet, umami, and bitter tastes are triggered by the binding of molecules to G protein-coupled receptors on the cell membranes of taste buds. Saltiness and sourness are perceived when alkali metal or hydrogen ions enter taste buds, respectively [4]. As taste senses both harmful and beneficial things, all basic tastes are classified as either aversive or appetitive, depending upon the effect the things they sense have on our bodies [5]. Sweetness helps to identify energy-rich foods, while bitterness serves as a warning sign of poisons [6].

For a long period, it was commonly accepted that there is a finite and small number of "basic tastes" of which all seemingly complex tastes are ultimately composed. As of the early twentieth century, physiologists and psychologists believed there were four basic tastes: sweetness, sourness, saltiness, bitterness. At that time umami was not proposed as a fifth taste but now a large number of authorities recognize it as the fifth taste [7]. In Asian countries within the sphere of mainly Chinese and Indian cultural influence, pungency (piquancy or hotness) had traditionally been considered a sixth basic taste. Today, the consensus is that sweet, amino acid (umami), and bitter taste converge

one common transduction channel, the transient receptor potential channel TRPM5, *via* phospholipase C (PLC). TRPM5 is a newly discovered TRP related to other channels in sensory signaling systems. It has been shown that PLC, a major signaling effect or of G-protein coupled receptors (GPCRs), and TRPM5 are co expressed with T1Rs and T2Rs and are vital for sweet, amino acid, and bitter taste transduction. Activation of T1R or T2R receptors by their respective taste molecules would stimulate G proteins, and in turn PLC (PLC- β 2). The activation of PLC generates two intracellular messengers -IP3 and di-acyl glycerol (DAG) - from the hydrolysis of phosphatidylinositol-4,5-bisphosphate (PIP2) and opens the TRPM5 channel, resulting in the generation of a depolarizing receptor potential. Other additional pathways may modulate sweet, amino acid, or bitter taste reception but would not, themselves, trigger a taste response. It is not at present known how PLC activates TRPM5 or whether DAG is involved [8-18].

1.1.1 Taste Masking

There are numerous pharmaceutical and over the counter (OTC) preparations that contain active ingredients, which are bitter in taste. With respect to OTC preparations, such as cough and cold syrups, the bitterness of the preparation leads to lack of patient compliance. Among examples that are commonly used drugs with bitter taste; pseudoephedrine, a sympathomimetic drug of the phenethylamine and amphetamine. It may be used as a nasal/sinus decongestant, as a stimulant, or as a wakefulness-promoting agent [19], dextromethorphan an antitussive (cough suppressant) drug. It is one of the active ingredients in many over-the-counter cold and cough medicines.

Dextromethorphan has also found other uses in medicine, ranging from pain relief to psychological applications. It is sold in syrup, tablet, spray, and lozenge forms. In its pure form, dextromethorphan occurs as a white powder [20], dyphylline also known as dipprophyllinea xanthine derivative with bronchodilator and vasodilator effects. It is used in the treatment of respiratory disorders like asthma, cardiac, and bronchitis. It acts as an adenosine receptor antagonist and phosphodiesterase inhibitor [21]. phenylephrine is a selective α_1 -adrenergic receptor agonist used primarily as a decongestant, as an agent

to dilate the pupil, and to increase blood pressure [22]. Phenylephrine is marketed as a substitute for the decongestant pseudoephedrine, chlorhexidine a chemical antiseptic. It is effective on both Gram-positive and Gram-negative bacteria, although it is less effective with some Gram-negative bacteria. It has both bactericidal and bacteriostatic mechanisms of action, the mechanism of action being membrane disruption, not ATPase inactivation as previously thought [23]. It is also useful against fungi and enveloped viruses, though this has not been extensively investigated, atorvastatin a member of the drug class known as statins, used for lowering blood cholesterol. It also stabilizes plaque and prevents strokes through anti-inflammatory and other mechanisms. Like all statins, atorvastatin works by inhibiting HMG-CoA reductase, an enzyme found in liver tissue that plays a key role in production of cholesterol in the body [22], loperamide a piperidine derivative, is an opioid drug used against diarrhea resulting from gastroenteritis or inflammatory bowel disease. In most countries it is available generically [24]. terfenadine was an antihistamine formerly used for the treatment of allergic conditions. It was brought to market by Hoechst Marion Roussel (now Sanofi-Aventis) and marketed under various brand names. According to its manufacturer, terfenadine had been used by over 100 million patients worldwide as of 1990 [25]. It was superseded by fexofenadine in the 1990s due to the risk of a particular type of disruption of the electrical rhythms of the heart (specifically cardiac arrhythmia caused by QT interval prolongation) [22], prednisolone is a synthetic glucocorticoid, a derivative of cortisol, which is used to treat a variety of inflammatory and auto-immune conditions. It is the active metabolite of the drug prednisone and is used especially in patients with hepatic failure, as these individuals are unable to metabolize prednisone into prednisolone [22], salbutamol, or albuterol (USAN) is a short-acting β_2 -adrenergic receptor agonist used for the relief of bronchospasm in conditions such as asthma and chronic obstructive pulmonary disease. It is marketed as Ventolin among other brand names. Salbutamol was the first selective β_2 -receptor agonist to be marketed – in 1968. It was first sold by Allen & Hanburys under the brand name Ventolin. The drug was an instant success, and has been used for the treatment of asthma ever since [26]. guaifenesin, or guaiphenesin (former BAN), also glyceryl guaiacolate, is

an expectorant drug sold over the counter and usually taken orally to assist the bringing up (expectoration) of phlegm from the airways in acute respiratory tract infections [22] and amoxicillin a moderate-spectrum, bacteriolytic, β -lactam antibiotic used to treat bacterial infections caused by susceptible microorganisms. It is usually the drug of choice within the class because it is better absorbed, following oral administration, than other β -lactam antibiotics. Amoxicillin is one of the most common antibiotics prescribed for children. The drug became available in 1972 [22].

1.1.2 Challenges and criteria for pursuing masking bitter taste approaches

The most significant challenges that facing developers when pursuing masking bitter taste drugs approaches are: (i) Safety, tolerability and efficacy of the compound which are based on non-clinical testing, and physicochemical properties such as solubility, permeability and stability, (ii) lack of robust and reliable techniques for early taste screening of compounds with limited toxicity data, (iii) structure–taste relationships of pharmaceutically active molecules is limited, (iv) The perception of taste of pharmaceuticals has been shown to be different between adults and children and it might differ between healthy and patient children [4] and (v) ethical concerns to perform taste studies in healthy children unless the study is a ‘swill and spit’ one with drugs known to have a good safety profile [27-29].

1.2 Bitter taste masking approaches (techniques)

A variety of taste masking approaches has been used to address the patient compliance problem. With strongly bad tasting medications even a little exposure is sufficient to perceive the bad taste. Conventional taste masking methods such as the use of sweeteners, amino acids and flavoring agents alone are often inadequate in masking the taste of highly bitter drugs. Drugs such as macrolide antibiotics, non-steroidal anti-inflammatory such as ibuprofen, quinine, celecoxib, etoricoxib, levofloxacin and penicillins have a pronounced bitter taste [30]. Masking the taste of water soluble bitter drugs, especially those given in high doses, is difficult to achieve by using sweeteners

alone. As a consequence, several approaches have been investigated and have resulted in the development of more efficient techniques for masking the bitter taste of active ingredients. All of the developed techniques are based on the physical modification of the formulation containing the bitter tastant. Among the approaches used to mask bitter taste of pharmaceuticals are: (1) taste masking using flavors, sweeteners, and amino acids. This technique is the foremost and the simplest approach for taste masking, especially in the case of pediatric formulations, chewable tablets, and liquid formulations. However, it is not an ideal to be used for highly bitter and highly water soluble drugs. An example for such approach is the use of monosodium glycyrrhizinate together with flavors to mask the bitter taste of guaiphenesin (an expectorant drug). Taste masked

lamivudine (antiretroviral drug) was prepared by using lemon, orange and coffee flavors [3,31]; (2) taste masking with lipophilic vehicles such as: i) Lipids; acetaminophen granules are sprayed with molten stearyl stearate, mixed with suitable tablet excipients, and incorporated into a taste masked, chewable tablet formulation and (ii) lecithin and Lecithin-like substances; formulations with lecithin or lecithin-like substances in large quantities are believed to efficiently mask bitter taste of pharmaceuticals [3]. An example of a drug formulation containing lecithin-like substance is the one composed of magnesium aluminum silicate with soybean lecithin and talampicillin HCl (antibiotic drug); (3) coating is one of the most efficient and commonly used taste masking techniques. It is more efficient technology for aggressively bitter drugs even though coating imperfections, if present, reduce the efficiency of the technique. Coating of tablets, pellets or any other kind of particles with a film-forming polymer is a successful approach to provide a physical barrier, concealing unpleasant odors and bitter taste. Additionally, it can prevent penetration of moisture into the formulation. Coating materials can be selected from a wide range of hydrophobic and hydrophilic polymers such as polyvinylpyrrolidone, polyvinyl alcohol and cellulose derivatives. The ideal polymer for taste-masking, odor suppression and moisture protection should prevent dissolution of the dosage form in the mouth, but should be readily soluble in the stomach. Coating is classified based on the type of coating material, coating solvent system, and

the number of coating layers. Taste masked famotidine (a drug for ulcer treatment) formulated by using a combination of water soluble polymers like polyvinylpyrrolidone and insoluble polymers like cellulose acetate is an example of such technique. Other various inert coating agents can be used to coat bitter drugs. These coating agents simply provide a physical barrier over the drug particles. Examples for such coating agents are starch, povidone, gelatin, methylcellulose, ethyl cellulose and etc. One of the most efficient Method of drug particle coating is the fluidized bed processor [4]. In this approach, powders as fine as 50 um are fluidized in an expansion chamber by means of heated, high-velocity air, and the drug particles are coated with a coating solution introduced usually from the top as a spray through a nozzle. Increasing the length of the coating cycle can increase coating thickness. Taste masking of Ibuprofen has been successfully achieved by this technique [4]; (4) microencapsulation is a technique applicable to protect materials from oxidation, volatilizing as well as to mask their bitter tastes [6]. Microencapsulation processes are commonly based on the principle of solvent extraction or evaporation. Microencapsulation as a process has been defined by Bakan [6] as a means of applying relatively thin coating to small particles of solid, droplets of liquid and dispersion. This process can be used for masking the bitter taste of drugs by microencapsulating drug particles with various coating agents. Coating agents employed includes gelatin, povidone, HPMC, ethyl cellulose, Bees wax, carnauba wax, acrylics and shellac. Bitter-tasting drugs can be first encapsulated to produce free flowing microcapsules, which are then blended with other excipients and compressed into tablets. Microencapsulation also increases the stability of the drug. It can be accomplished by a variety of methods, including air suspension, coacervation-phase separation, spray drying and congealing, pan coating, solvent evaporation and multi-orifice centrifugation techniques; (5) taste suppressants and potentiators such as the Linguagen's bitter blockers (e.g. adenosine monophosphate) are used for masking bitter taste of various compounding by competing with the latter on binding to the G-protein coupled receptor sites (GPCR) [32]; (6) ion exchange resins are water insoluble, cross-linked polymers containing salt forming groups in repeating position on the polymer chain. Drug can be bound to the ion exchange resin by either repeated exposure of the resin to the drug in a

chromatographic column or by prolonged contact of resin with the drug solution. The resins forms insoluble adsorbates or resinates through weak ionic bonding with oppositely charged drugs. The exchange of counter ions from resin is competitive. Most of the bitter drugs have amine as a functional group, which is the cause of their obnoxious taste. If the functional groups are blocked by complex formation the bitterness of the drug reduces drastically. A drug- resin complex is made from the bitter drugs and ion - exchange resins. The nature of the drug- resin complex is such that the average pH of 6.7 and cation concentration of about 40 meq/ lit in saliva are not able to break the drug- resin complex but it is weak enough to be broken down by the hydrochloric acid present in the stomach. Thus the drug: resin complex is absolutely tasteless and stable, with no after taste, but at the same time its bioavailability is not affected. Ion exchange resin like Amberlite was used to formulate taste masked fast dissolving orally consumable films of dextromethorphan (cough suppressant drug) [33,34]; (7) inclusion complexes in which the drug molecule fits into the cavity of a complexing agent forming a stable complex. The obtained complexing agent has the potential to mask the bitter taste of a drug by either decreasing its oral solubility on ingestion, or decreasing the amount of drug particles exposed to taste buds, thus reducing the perception of bitter taste. The inclusion complexes with cyclodextrin owe their existence to van der Waals forces between the host and guest. Cyclodextrin is the most widely used complexing agent for inclusion type complexes. It is a sweet, nontoxic, cyclic oligosaccharide derived from starch. Cyclodextrin forms inclusion complexes with organic molecules both in solid state and in solution [35]; (8) pH modifiers are capable of generating a specific pH microenvironment in aqueous media that has the ability to facilitate *in situ* precipitation of the bitter drug compound in saliva thus reducing the overall taste sensation for liquid dosage forms like suspension [36]; (9) adsorbates which are commonly used with other taste masking technologies to mask pharmaceuticals bitterness. The pharmaceutical may be adsorbed or/and entrapped in the matrix of the adsorbate porous, which may result in a delayed release of the bitter tastant during the passage through the oral cavity and hence achieving taste masking [37]; (10) chemicals; the solubility and absorption of drugs can be modified by the formation of molecular complexes. Lowering drug solubility through

molecular complexation can decrease the intensity of bitterness. Higuchi and Pitman [38] reported that caffeine forms complexes with organic acids that are less soluble than xanthenes and as such can be used to decrease the bitter taste of caffeine; (11) solid dispersions; solid dispersion have been defined as dispersion of one or more active ingredients in an inert carrier or matrix at solid state prepared by melting (fusion) solvent or melting solvent method. Solid dispersion is also called as co precipitates for those preparation obtained by solvent method such as co precipitates of sulphathiazole and povidone. Solid dispersions using insoluble matrices or bland matrices may be used to mask the bitter taste of drugs. Also using them as absorbates on various carriers may increase the stability of certain drugs [39]; (12) multiple emulsions; a novel technique for taste masking of drugs employing multiple emulsions has been prepared by dissolving drug in the inner aqueous phase of w/o/w emulsion under conditions of good shelf stability. The formulation is designed to release the drug through the oil phase in the presence of gastrointestinal fluid [40]; (13) using liposomes is another way of masking the unpleasant taste of therapeutic agent is to entrap them into liposome.

1.3 Human bitter taste receptors

Within the oral cavity bitter substances are released from foodstuff resulting in the activation of one or several of the ~25 functional human bitter taste receptors of the taste 2 receptor family (TAS2R), that belongs to the large family of G protein-coupled receptors (GPCRs) [43]. Previous screening efforts of heterologously expressed human TAS2Rs resulted in the deorphanization of 21 out of the 25 receptors [44]. The ability to associate the majority of TAS2Rs with activating bitter substances revealed several important features of the TAS2R gene family. Firstly, a single bitter compound can activate multiple TAS2Rs and, vice versa, TAS2Rs can respond to several bitter substances. Secondly, the TAS2Rs' agonist recognition profiles range from broadly to narrowly-tuned. A recent screening experiment using more than 100 natural and synthetic bitter compounds demonstrated that the three most broadly tuned receptors TAS2R10, TAS2R14, and TAS2R46 each recognized about one-third of the tested substances, and that their combined response profiles accounted for the detection of already one-half of

all substances [45]. Hence, these receptors may contribute disproportionately to human bitter tastant recognition. Two of these receptors, the TAS2R46 and the TAS2R10, have been subjected to detailed structure-function analyses to elucidate the architecture of their binding pockets which enable the recognition of so many structurally different bitter substances while maintaining a high level of selectivity. It was shown that these TAS2Rs possess single ligand binding pockets tailored to recognize multiple diverse bitter agonists [46]. Although TAS2R14 has been among the first deorphanized TAS2Rs, similar experiments for this receptor are lacking. In fact, the original report already recognized that this receptor may exhibit an exceptionally broad tuning, with no apparent common chemical motifs among the identified agonists. By combined *in silico* prediction of potentially agonistic molecules and subsequent functional screening of candidate agonists, numerous additional and previously unknown activators of TAS2R14 were revealed. The data suggested that, instead of a single common pharmacophore, a number of different chemical scaffolds may exist among TAS2R14 agonists. Moreover, it turned out that a considerable number of the newly identified agonists of this receptor represent important drugs with anti-inflammatory, analgesic, and anti-tumor activities [47]. Knowledge about the chemical features of agonists is of utmost importance for identifying potential off-target activities of medical drugs. The fact that TAS2R14 is the most abundant TAS2R in human heart tissue [48], underscores the importance for a precise knowledge on structure-activity relationships among its agonists. Moreover, an improved knowledge about chemical structures common to agonists may help to repurpose existing drugs, or rationally design novel TAS2R14 antagonists. Although at present only few reasonably specific TAS2R antagonists have been identified, the majority of these molecules share common chemical structures with the corresponding receptor agonists [49].

To elucidate the structural requirements for TAS2R14 agonists and to probe the size of the TAS2R14 binding pocket we performed functional calcium imaging experiments. In contrast to previous studies, which mostly relied on testing commercially available compounds, we tailored novel test compounds, based on known agonists, by chemical syntheses [50]. The agonist activities of the newly synthesized substances were

determined and directly compared with those of the corresponding mother substances. Density functional theory (DFT) and modeling computational methodologies were integrated to analyze the results. This approach allowed the investigation of binding pocket requirements in an extraordinary broadly tuned receptor with great precision.

Table (1): Specific area of tongue.

Taste	Area of tongue
Sweet	Tip
Salt	Tip and Sides
Sour	Sides
Bitter	Back

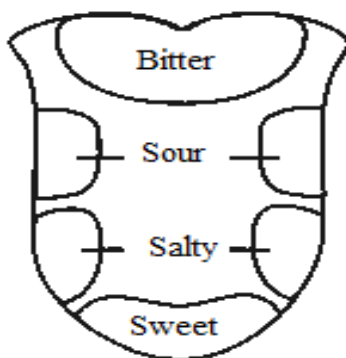


Figure (1): Locations of taste sensors on the tongue

Taste is an important issue for orally administered drugs; one of the most serious problems for drug formulation is the undesirable drug's taste. Drugs bitterness might reduce patient compliance thus decreasing therapeutic effect especially in children patients. Therefore, masking the bitter taste of a drug is an important issue in the pharmaceuticals industry.

1.4 General Objective

The main goal of this thesis was to synthesize, characterize novel bitter tastants derivatives: diclofenac hexyl and benzyl, mefenamic hexyl, decyl and benzyl, bezoin hexyl and benzyl aiming to understand the nature and the mode in which bitter taste receptor 14 activates bitter tastants.

Specific objectives:

- 1- To synthesize, characterize the following novel derivatives: diclofenac hexyl and benzyl, mefenamic hexyl, decyl and benzyl, bezoin hexyl and benzyl.
- 2- To study the agonist effect of the derivative towards bitter receptor 14.

Literature Review

Chapter Two

2. Literature Review

2.1. Bitter taste masking:

In 2011, Aditi Tripathi et al. declared that taste is an important parameter in case of drugs administering orally. Taste masking becomes a prerequisite for bitter drugs to improve the patient compliance especially in the pediatric and geriatric population. The problem of bitter taste of drug in pediatric formulations is a challenge to the formulators in the present scenario. Masking the bitter taste of drugs is a potential tool for the improvement of patient compliance which intern decides the commercial success of the product. Two approaches are commonly utilized to overcome the bad taste of the drug. The first includes reduction of drug solubility in the saliva and the second approach is to alter the ability of the drug to interact with taste receptor. Various methods are available to mask the undesirable taste of the drugs. Some of them are coating of drug particles, by formation of inclusion complexes, molecular complexes of drugs with other chemicals, solid dispersions, melting method, micro encapsulation, prodrugs, mass extrusion methods and ion exchange resins [51].

In 2007, Shagufta Khan et al. have studied approaches to mask the bitter taste of ondansetron. The purpose of their research was to mask the intensely bitter taste of ondansetron HCl and to formulate a rapid disintegrating tablet (RDT) of the taste-masked drug. Taste masking was done by complexing ondansetron HCl with aminoalkyl methacrylate copolymer (Eudragit EPO) in different ratios by the precipitation method. Drug-polymer complexes (DPCs) were tested for drug content, in vitro taste in simulated salivary fluid (SSF) of pH 6.2, and molecular property. Complex that did not release drug in SSF was considered taste-masked and selected for formulation RDTs. The complex with drug-polymer ratio of 8:2 did not show drug release in SSF; therefore, it was selected. The properties of tablets such as tensile strength, wetting time, water absorption ratio, in vitro disintegration time, and disintegration in the oral cavity were investigated

to elucidate the wetting and disintegration characteristics of tablets. Polyplasdone XL-10 7% wt/wt gave the minimum disintegration time. Tablets of batch F4 containing spray-dried mannitol and microcrystalline cellulose in the ratio 1:1 and 7% wt/wt Polyplasdone XL-10 showed faster disintegration, within 12.5 seconds, than the marketed tablet (112 seconds). Good correlation between in vitro disintegration behavior and in the oral cavity was recognized. Taste evaluation of RDT in human volunteers revealed considerable taste masking with the degree of bitterness below threshold value (0.5) ultimately reaching to 0 within 15 minutes, whereas ondansetron HCl was rated intensely bitter with a score of 3 for 10 minutes. Tablets of batch F4 also revealed rapid drug release (t_{90} , 60 seconds) in SGF compared with marketed formulation (t_{90} , 240 seconds; $P < .01$). Thus, results conclusively demonstrated successful masking of taste and rapid disintegration of the formulated tablets in the oral cavity [52].

2.2 Selected Drugs

2.2.1 Mefenamic acid

In 2007, Dev. et al. have synthesized mefenamic acid- β -cyclodextrin prodrug. The primary hydroxy group of β - cyclodextrins was used to block the free acid group of mefenamic acid. The synthesis consisted of several protection and deprotection steps. The study demonstrated that mefenamic acid- β -cyclodextrin prodrug has retained its pharmacological activity as was evident by the percentage inhibition of edema and in acetic acid induced writhing method and comparison with the activity of its active parent drug. In addition, the study showed that the maximum activity of the ester prodrug was obtained after 6 hours indicating that there is no drug absorption in the stomach. Further, in vitro studies showed the ester was completely stable in simulated gastric and intestinal fluid whereas it underwent complete hydrolysis in rat fecal contents representing the colon. Ulcerogenicity studies showed that the ester prodrug is not ulcerogenic indicating that masking the carboxyl group in mefenamic acid is a good approach to reduce the ulcerogenicity, a major side effect of the active parent drug, mefenamic acid [53].

2.2.2 Diclofenac sodium

Taste masking of diclofenac sodium using microencapsulation, were successfully prepared using a system of ethylcellulose (EC)-toluene-petroleum ether. The prepared microcapsules were taste evaluated by a taste panel of 10 volunteers. Microcapsules containing PEG 20% or DEP 40% showed a faster rate of DS release compared to that obtained from other microcapsules and crushed commercial enteric coated tablets (Voltaren). The palatability and the taste of DS were significantly improved by microencapsulation. The extent of taste masking was influenced by the microcapsule core: wall ratio, the presence of additives within the core, the type and concentration of plasticizer and initial core size [54].

Bitter taste of diclofenac sodium by formulate an orally-disintegrating tablet (ODT) to achieving effective taste masking include various physical and chemical methods that prevent the drug substance from interaction with the taste buds. Veegum (magnesium aluminum silicate) as the taste masking agent and sodium starch glycolate and croscarmellose sodium as superdisintegrants. Granules of diclofenac sodium were prepared using different ratios of veegum (1:0.5, 1:1, 1:1.5, 1:2) by wet granulation method and evaluated for pre-compression parameters. Concluded that taste masked diclofenac sodium fast disintegrating tablets can be successfully prepared using veegum as a taste masking agent (1:1.5) and the sodium starch glycolate and croscarmellose sodium (5%) as superdisintegrants [55].

Experimental

Chapter three

3. Materials and Methods

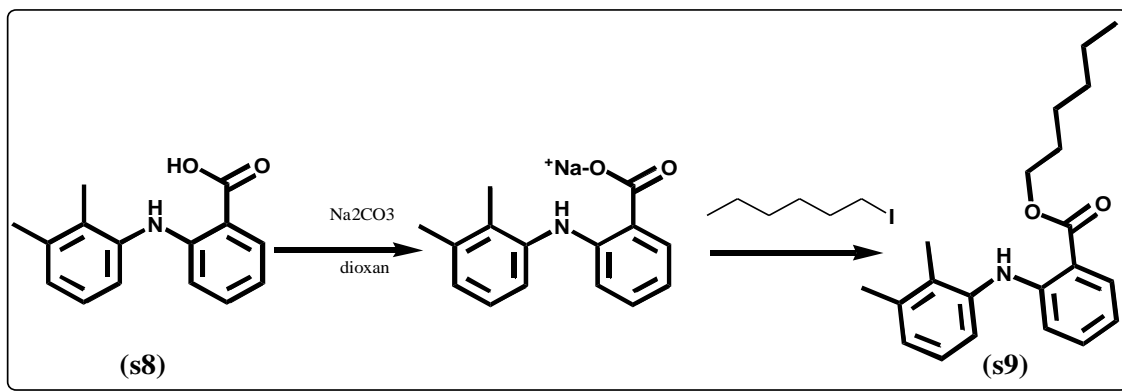
3.1. Chemical syntheses and analysis

Inorganic salts were of analytical grade and were used without further purification. Organic buffer components were distilled or recrystallized. Distilled water was redistilled twice before use from all-glass apparatus. Benzoin, diclofenac sodium, mefenamic acid, iodohexane, iododecane, benzyl bromide, sodium hydride, sodium hydroxide, hydrochloric acid, sodium carbonate, anhydrous MgSO₄, dioxane, dimethylformamide and ethyl acetate were purchased from Aldrich Chemicals Ltd and were used without further purification. HPLC grade solvents of methanol, acetonitrile and water were purchased from Sigma Aldrich. High purity dichloromethane, THF and diethyl ether (> 99%) were purchased from Biolab (Israel). Silica gel (Silica gel 60 (0.040-0.063 mm)), thin layer chromatography (TLC) (TLC Silica gel 60 F254) sheets were purchased from Merck Ltd. The LC/ESI-MS/MS system used was Agilent 1200 series liquid chromatography coupled with a 6520 accurate mass quadrupole-time of flight mass spectrometer (Q-TOF LC/MS). The analysis was performed in the positive electrospray ionization mode. The capillary voltage was 4.0 kV, the scanned mass range was 200-540 *m/z* (MS). The high pressure liquid chromatography (HPLC) system consisted of an Alliance 2695 module equipped with 2996 Photodiode array detector from Waters (Germany). Data acquisition and control were carried out using Empower 2™ software (Waters, Germany). Analytes were separated on a 4.6 mm x150 mm XBridge® C18 column (5 μm particle size) used in conjunction with a 4.6 x 20 mm, XBridge® C18 guard column. Microfilters of 0.45 μm porosity were normally used (Acrodisc® GHP, Waters). pH meter model HM-30G: TOA electronics™ was used in this study to measure the pH value for the buffers. The Sep-Pack C18 6cc (1 g) cartridges were purchased from Waters (Milford, MA, USA). ¹H-NMR experiments were performed with a Bruker AvanceII 400 spectrometer equipped with a 5 mm BBO probe. Infrared spectra (FTIR) for solid compounds were obtained from a KBr matrix and for liquid compounds as neat (4000–400 cm⁻¹) using a PerkinElmer Precisely, Spectrum 100.

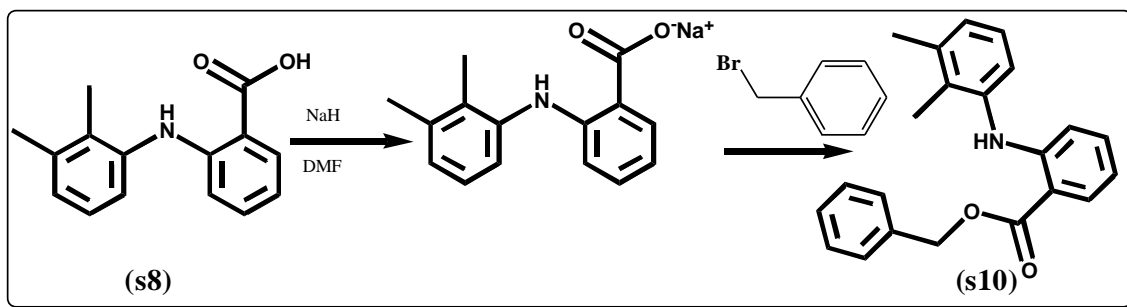
3.2 Synthesis of bitter taste derivatives

3.2.1 Preparation of mefenamic acid, and diclofenac alkyl esters

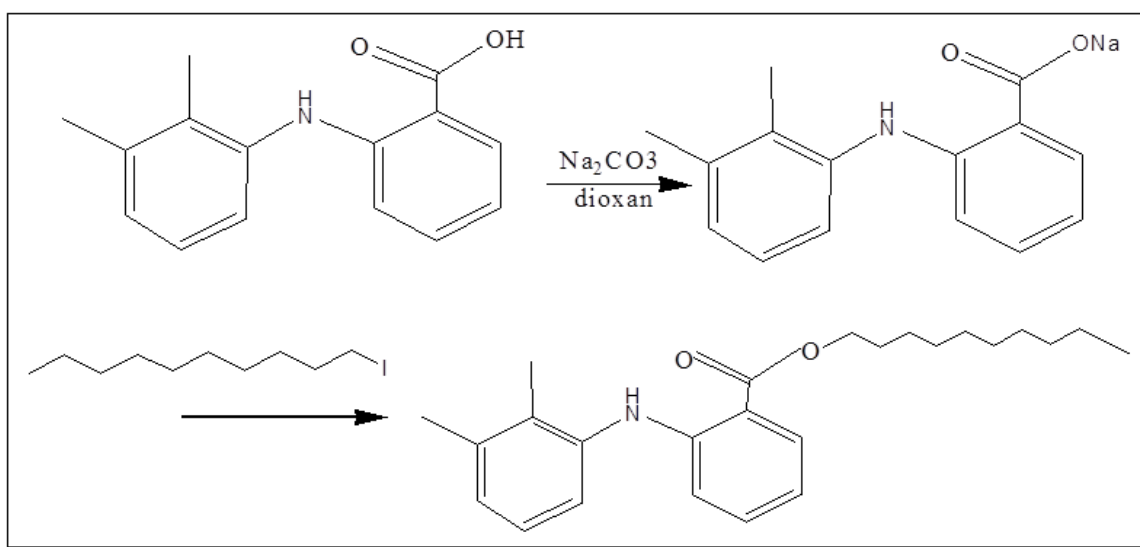
In a 250 mL round-bottom flask, diclofenac sodium or mefenamic acid (10 mmol) was dissolved in dry dioxane (50 mL), solutions of 2 gram sodium carbonate in dry dioxane (50 ml) and 40 mmol alkyl halide (1-iodohexane, 1-iododecane or benzyl bromide) in dry dioxane (50 ml) were added, the resulting solution was refluxed while stirring for 3 days (Schemes 1-3). The reaction mixture was cooled to room temperature and evaporated using vacuum pump to dryness. 50 ml 1N HCl and 50 ml dry ether were added to the dry mixture, the resulting mixture was transferred to separator funnel and shaken. The two layers were separated and the acidic aqueous layer was extracted twice with dry ether (50 ml). The combined ether fractions were dried over $MgSO_4$ anhydrous, filtered and evaporated to dryness using vacuum pump. The dry residue was subjected to column chromatography and the desired product was dried and characterized by FTIR, H-NMR and LC-MS analysis (see supporting information).



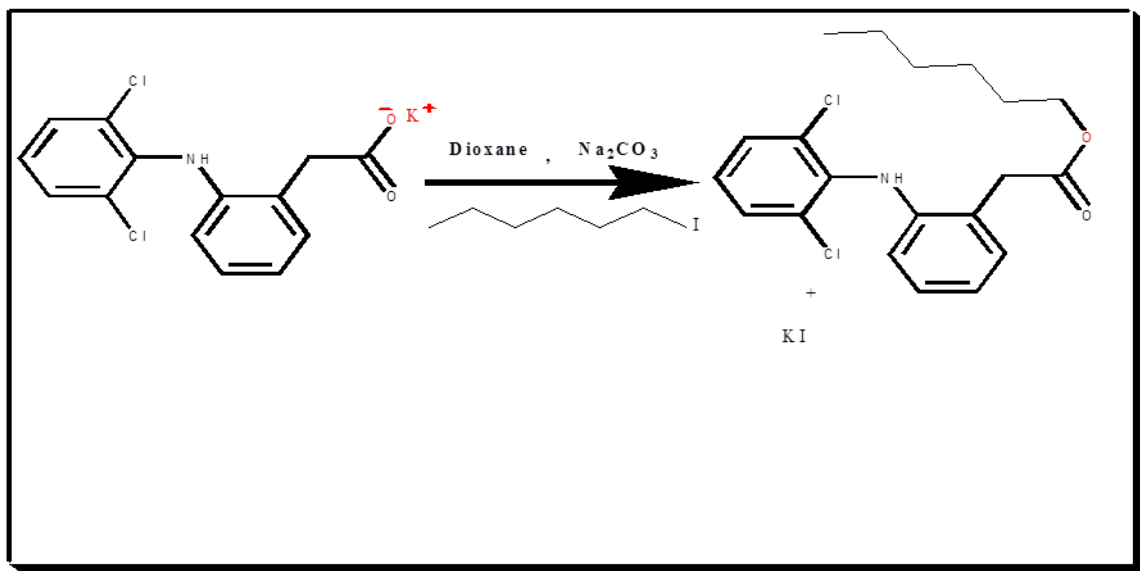
Scheme 1: Synthesis of mefenamic hexyl derivative S9



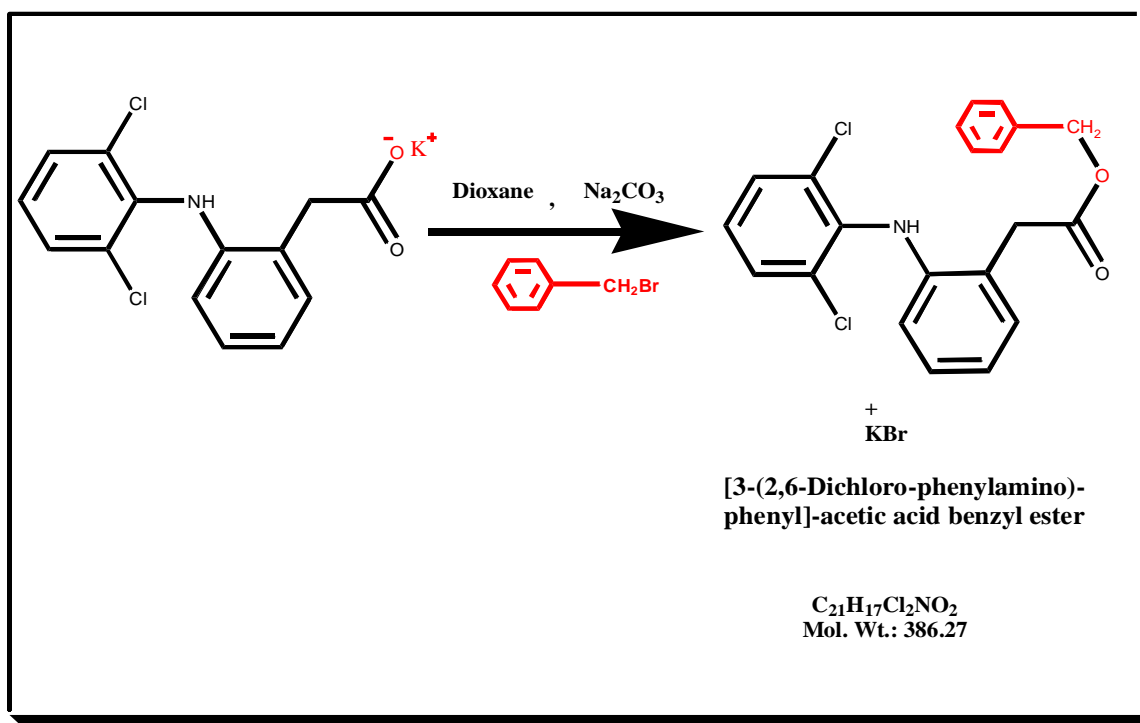
Scheme 2: Reaction of mefenamic acid with benzyl bromide to produce derivative S10:



Scheme 3: Reaction of mefenamic acid with 1-iododecane to produce derivative.



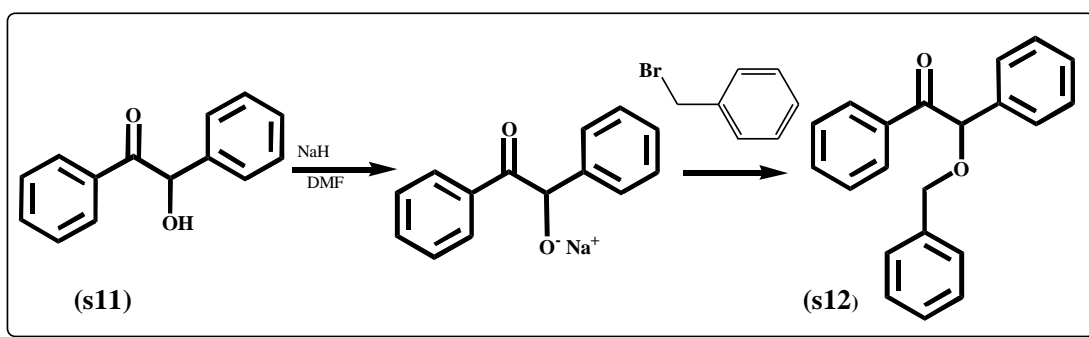
Scheme 4: Synthesis of diclofenac hexyl ester derivative via reacting diclofenac sodium with 1-iodohexane.



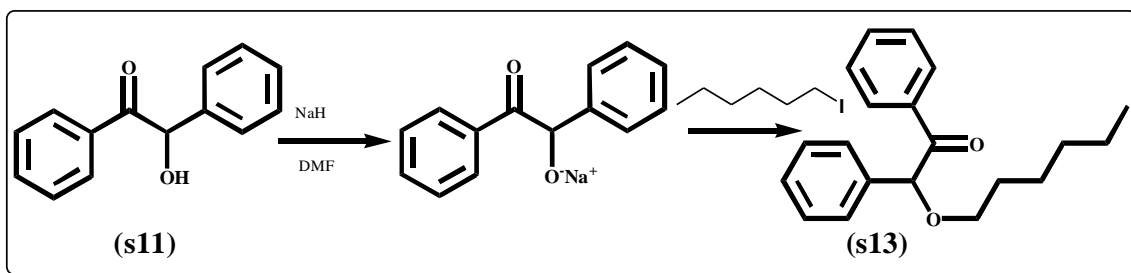
Scheme 5: Synthesis of diclofenac benzyl ester derivative via reacting diclofenac sodium with benzyl bromide.

3.2.2 Preparation of benzoin alkyl ethers

In a 250 ml round-bottom flask, benzoin (10 mmol) was dissolved in dry dioxane (50 mL), 60% sodium hydride (30 mmol) was added to the solution, the reaction was stirred at room temperature until hydrogen gas production ended, benzyl bromide or hexyl iodide (20 mmol) was slowly added and the reaction was mixed for overnight and then refluxed for two hours (Schemes 4-5). The reaction mixture was cooled to room temperature, few drops of 0.1 N HCl were added slowly to destroy the excess of sodium hydride and then the reaction mixture was evaporated to dryness. 1N NaOH (50 ml) and dry ether (50 ml) were added to the dry mixture; the resulting mixture was transferred to separator funnel and shaken. The two layers were separated and the basic aqueous layer was extracted twice with dry ether (50 ml). The combined ether fractions were dried over MgSO₄ anhydrous, filtered and evaporated to dryness using vacuum pump. The dry residue was subjected to column chromatography and the desired product was dried and characterized by FTIR, H-NMR and LC-MS analysis (see supporting information).



Scheme 6: Reaction of benzoin with benzyl bromide to produce S12



Scheme 7: Reaction of benzoin with iodohexane to produce S13

3.3 Functional calcium imaging experiments

Functional heterologous expression of TAS2R14 was done as previously reported [6, 7, 11]. Briefly, TAS2R14 cDNA cloned in frame with a 5' located sequence coding for the first 45 amino acids of rat somatostatin receptor 3 and a 3' located sequence coding for the herpes simplex virus glycoprotein D epitope in the vector pcDNA5FRT was transiently transfected into HEK 293T-G α 16gust44 cells. After a ~24 h incubation period cells were loaded with Fluo-4 AM in the presence of 2.5 mM probenecid, then washed several times with C1-buffer and placed in a fluorometric imaging plate reader. After application of test stimuli changes in fluorescence were monitored. As negative controls cells transfected with an empty expression vector were used and directly compared to receptor transfected cells.

3.4. Computational analyses

QM studies - The Becke three-parameter, hybrid functional combined with the Lee, Yang, and Parr correlation functional, denoted B3LYP, were employed in the calculations using density functional theory (DFT). All calculations were carried out based on the restricted Hartree-Fock method using the quantum chemical package Gaussian-2009 [21]. The starting geometries of all calculated molecules were obtained using the Argus Lab program [22] and were initially optimized at AM1, PM3, HF/6-31G level of theory, followed by optimization at the B3LYP/6-31G(d,p). The search for the global minimum structure in the mefenamic acid and diclofenac derivatives studied was accomplished by 36 rotations of the alkoxy group about the C-C-Ar in increments of 10°, and calculation of the energies of the resulting conformers. An energy minimum (a stable compound or a reactive intermediate) has no negative vibrational force constant. In case of the benzoin derivatives, 36° rotations of the alkyl group about the etheric C-O bond in increments of 10°, and calculation of the energies of the resulting conformers were conducted.

3.5 Homology modeling

β 2 adrenergic receptor (PDB ID: 3SN6) [23] was used as template for constructing TAS2R14 model. Sequence alignment was performed with MP-T [24] and manually adjusted; homology modeling was carried out with MEDELLER [25]. Hydrogen atoms and side chain orientations of the receptor were optimized at physiological pH with the Protein Preparation Wizard tool in Maestro (version 10.2, Schrödinger, LLC, New York, NY, 2014) and the Predict Side Chains tool in Prime (version 4.0, Schrödinger, LLC, New York, NY, 2014), respectively. Throughout the article, transmembrane (TM) residues are identified by a superscript number system according to the Ballesteros-Weinstein numbering method [26].

3.6 Docking

Ligands were manually built using the Built facility in Maestro (version 10.2, Schrödinger, LLC, New York, NY, 2014). 3D structures, stereoisomers, tautomers and protomers at pH 7.0 ± 0.5 were generated with LigPrep (version 4.0, Schrödinger, LLC, New York, NY, 2014). Glide (Grid-based Ligand Docking with Energetics) software (version 6.7, Schrödinger, LLC, New York, NY, 2014) was used for the Induced Fit Docking [27, 28]. The grid box was centroid of residues Trp 89 and Phe 247, and the van der Waals scalings of receptors and ligands were 0.5. Side chains of residues within 5.0 Å of the ligand were refined. The docking was performed with the Standard Precision (SP) mode of Glide. Docking poses showing similar binding modes among all compounds were selected and re-scored with the Extra Precision (XP) mode of Glide. In the case of the diclofenac derivatives, the binding poses were obtained aligning the ligand structures to the diclofenac in its docking pose with Phase Shape Screening (Phase, version 4.3,

Schrödinger, LLC, New York, NY, 2014). Then the resulting complexes between TAS2R14 and diclofenac derivatives were first minimized with MacroModel (version 10.8, Schrödinger, LLC, New York, NY, 2014) to a derivative convergence of 0.05 kJ/mol-Å using the Polak-Ribiere Conjugate Gradient (PRCG) minimization algorithm, the OPLS2005 force field and the GB/SA water solvation model; and then used as input for Glide Pose Refinement. Glide XP was used as scoring function for all complexes (see Table 2).

Results and Discussion

Chapter Four

4. Results and Discussion

4.1 Characterization

Mefenamic acid (2-(2,3-dimethylphenyl) aminobenzoic acid) and diclofenac (2-(2,6-dichloranilino) phenylacetic acid) have been identified as novel TAS2R14 agonists in a recent *in silico* screening of agonists and confirmed by functional assays. Both substances represent non-steroidal anti-inflammatory drugs and are structurally similar to flufenamic acid, a previously identified TAS2R14 agonist which was used as a template for the *in silico* prediction of a ligand-based pharmacophore model. Benzoin (2-hydroxy-1,2-di(phenyl)ethanone), which represents the most simple aromatic hydroxyl ketone and is a natural component in bitter almond oil, also belongs to the group of cognate TAS2R14 agonists sharing the presence of two phenyl ring systems with mefenamic acid and diclofenac (Fig. 2) [6,11].

To analyze structural requirements of TAS2R14 agonists we first modified the most potent of the 3 agonists, mefenamic acid, by the addition of a third phenyl group linked to the carboxyl group via an ester bond (Fig. 2) and tested the compound in functional assays. Surprisingly, the resulting mefenamic acid benzyl ester retained agonistic properties, although the lack of receptor activation below a concentration of 10 μM indicates reduced potency (Fig. 3A). The occurrence of receptor-independent calcium signals already at 30 μM prevented the use of higher compound concentrations in this assay. The addition of an aliphatic group with an identical number of carbon atoms, leading to mefenamic acid hexyl ester, similarly resulted in a moderate reduction of the potency, yet, receptor responses were not abolished (Fig. 3A). Even the compound mefenamic acid decyl ester robustly activated TAS2R14-expressing cells starting from a concentration of ~ 100 μM (Fig. 3A). Thus, for a potent agonist such as mefenamic acid, the substantial increase of the molecular mass somewhat impairs TAS2R14 activation, but does not lead to a loss of activation. To determine whether chemical modification of

the structurally-related, but less potent agonist diclofenac shows similar tolerance, we tested the corresponding benzyl and hexyl esters of this compound as well. As evident from (Fig. 2B), diclofenac derivatives fail to activate TAS2R14 transfected cells at all applicable concentrations. Hence, performing the same modifications in agonists with lower potency resulted in pronounced changes in receptor activation.

Functional heterologous expression assays do not allow assessing binding of agonist molecules to receptors. Instead, receptor activation is monitored. To test whether the lack of TAS2R14 activation by diclofenac benzyl ester has resulted from a loss of its receptor binding capacity or whether steric hindrance has prevented occupation of the receptor's binding pocket by the compound, we set up competition experiments using the potent TAS2R14 agonist aristolochic acid [6,29]. We reasoned that, if diclofenac benzyl ester would not fit into the receptor's binding pocket, aristolochic acid treatment of TAS2R14 expressing cells should result in unimpaired receptor responses. If, however, diclofenac benzyl ester is able to enter the binding pocket without causing receptor activation, competitive inhibition of aristolochic acid activation should occur. We therefore challenged TAS2R14 expressing cells with increasing concentrations of diclofenac benzyl ester in the presence of a signal saturating concentration of aristolochic acid (3 μM) and monitored calcium responses. The calcium traces of aristolochic acid treated TAS2R14 expressing cells (Fig. 3C) showed no reduction of maximal amplitudes even in the presence of 100 μM diclofenac benzyl ester excluding the possibility that this compound acts as an inhibitory ligand (antagonist) for the receptor.

To confirm and extend the above observations, we modified benzoin, a TAS2R14 agonist with an even lower potency compared to diclofenac. Much to our surprise, the addition of aliphatic hexyl or aromatic benzyl side chains resulted in the generation of more potent agonists. For both benzoin derivatives we observed robust receptor responses already at concentrations of 10 μM , whereas the necessary concentration of unmodified benzoin required to activate TAS2R14 was \sim 10-fold higher (Fig. 4). Hence, despite the

pronounced chemical similarities between mefenamic acid, diclofenac and benzoin, it appears that their binding modes differ.

To gain further insight in the binding site of TAS2R14 bitter taste receptor, we performed computational analyses on ligand structures, receptor structure and ligand-receptor interactions, aiming to identify the chemical structural factors associated with TAS2R14 activation. Ground state structures (global minimum) for mefenamic acid, diclofenac, benzoin and their derivatives were calculated using QM approaches. Mefenamic acid and diclofenac show an intramolecular H-bond between the alkoxy group and the aniline nitrogen, not present in the benzoin structure. For mefenamic acid and diclofenac derivatives, two types of conformations were considered: one in which the alkoxy group is pointing towards the aniline nitrogen and another in which it is pointing far from it. It was found that the global minimum structures for the mefenamic acid derivatives all reside in a conformation where the alkoxy group is pointing far from the aniline nitrogen, except for mefenamic acid benzyl ester (Fig. 3A), whereas the global minimum structures for the diclofenac derivatives resided in a conformation where the alkoxy group is pointing towards the aniline nitrogen (Fig. 3B). Similarly, for the benzoin derivatives two types of conformations were considered: one in which the alkyl group is pointing towards the carbonyl group and another in which it is pointing far from it. It was found that the global minimum structures for all benzoin derivatives reside in a conformation where the alkyl group is pointing far from the carbonyl group (Fig. 4). The compounds with global minima with the substituent positioned far from the core of the compound skeleton structure (aniline nitrogen or carbonyl group), such as mefenamic acid hexyl, mefenamic acid decyl esters, benzoin benzyl and benzoin hexyl ethers, cause the activation of TAS2R14 to a variable extent, while the compounds with global minima for which substituent is placed near the structural core of the compound, such as in diclofenac benzyl and diclofenac hexyl esters, did not activate TAS2R14. Therefore, the difference between the mefenamic acid and benzoin derivatives on the one hand and the diclofenac derivatives on the other hand can be attributed to steric effects: the three dimensions of the ligands (dimensions A, B, and C, see Figs. 3 and 4) were calculated for

the different derivatives and demonstrate that the dimension B for diclofenac benzyl and diclofenac hexyl esters (11.85 Å and 11.69 Å, respectively) are much higher than that of all other derivatives (6.23-6.95 Å). It is worth noting that although the benzyl group in mefenamic acid benzyl ester is placed not far from the structure's core (aniline nitrogen) of the ester, it resides in a compact conformation (for DFT calculated global minimum structures for the tested compounds, see supplemental file 1).

To evaluate the ability of the compounds to interact with the receptor's binding pocket, compounds were docked into a TAS2R14 homology model based on the β 2 adrenergic receptor (PDB ID: 3SN6) [23] (Fig. 5). Mefenamic acid establishes π - π interactions with His94^{3.37}, Phe186^{5.46} and Phe243^{6.51}, and H-bonds with Asn93^{3.36} and Gln266^{7.39} side chains of TAS2R14 (Fig. 6A). Mefenamic acid derivatives interact with the receptor with a similar binding mode, but to accommodate the ester moiety; they are shifted compared to the original molecule (Fig. 6D and G): because of the ester substitution, interaction with Gln266^{7.39} is not possible and, because of the increased size, ligands cannot engage in all stacking interactions observed for mefenamic acid. Interestingly, in case of the mefenamic acid benzyl ester, the additional aromatic ring can re-establish one of these interactions, with improved activity compared to the other derivatives.

Diclofenac has a methyl spacer between the carboxyl group and the aromatic ring, and has chloride atoms in ortho positions of the phenyl group (Fig. 2). These structural modifications affect the binding mode: the carboxyl can interact with Asn93^{3.36} but not with Gln266^{7.39}; His94^{3.37}, establishes both hydrophobic and polar interactions with the ligand, but there is no interaction with Phe186^{5.46} (Fig. 6B). Since the methyl spacer is causing a shift in diclofenac binding, the addition of the ester moiety could increase steric hindrance, negatively affecting binding. Docking results of diclofenac derivatives did not furnish any poses comparable to the diclofenac pose described above. Diclofenac derivatives were also aligned to diclofenac in its docking conformation, and then minimized to adjust the position of the alkoxy group. Both the hexyl and the benzyl esters have clashes with the backbone of TM7. In particular, bad contacts were observed

between the hydrogen of the ligand alkoxy groups and the backbone Ile262^{7,35} (shown as red arrows in the 2D representation of binding modes in (Fig. 5E and H). This is despite diclofenac derivatives being closer to TM3 than other compounds (see the 3D representation of binding modes in (Fig. 5E and H). Thus, diclofenac derivatives cannot be accommodated in the binding pocket because of steric hindrance.

Benzoin and its derivatives were synthesized and tested in racemic mixture. The docking results of the R stereoisomers (R)-benzoin, (R)-benzoin benzyl ester and (R)-benzoin hexyl ester, showed better performance and are reported here. (R)-benzoin establishes an H-bond with Asn93^{3,36} and aromatic interactions with Trp89^{3,32} and Phe247^{6,55} (Fig. 5C). Interestingly, the benzoin derivatives can interact also with His94^{3,37} (Fig. 6F and I). In addition, the Mulliken atomic charges for benzoin, benzoin benzyl ether and benzoin hexyl ether, calculated by both DFT and AM1 methods, demonstrate that the net negative charge value around the two oxygen atoms in both ethers is higher than in benzoin, enabling these oxygens to participate in stronger interactions than in benzoin. This is in agreement with the functional data showing that ether derivatives being more potent agonists than benzoin.

4.2. Discussion

The TAS2R14 is a highly promiscuous human bitter taste receptor [6,10]. The wide tuning breadth of the receptor may be achieved by architecture of the ligand binding pocket that provides a diverse array of contact points for ligand interactions as well as sufficient space to accommodate the various agonists. Moreover, as we have shown for the broadly tuned human bitter taste receptor TAS2R10, the ability to interact with many structurally diverse bitter substances may come with the trade-off of rather low-affinity binding between receptor and agonist [9]. In order to characterize the binding pocket of TAS2R14 in more detail, we chemically synthesized derivatives of known TAS2R14 agonists and determined their ability to activate cells heterologously expressing the receptor. This approach demonstrated that TAS2R14 tolerated the additions of large chemical groups to the chemical backbone of ligand molecules or, in case of the benzoin

derivatives, even showed improved activation. This suggests that the TAS2R14 binding pocket is wide with few size constraints for agonists. Moreover, ligands are not only required to establish contacts within the receptor binding pockets, they first need to gain access through extracellular loops which are decorated with at least one, and in case of TAS2R14, with two, asparagine-linked, oligosaccharide side-chains [30]. Sequence deviation from crystallized GPCRs prevents reliable inclusion of loops in homology models and hence, understanding of the constraints for entering the binding pocket. Nevertheless, previous observations [8, 31] indicate that receptor residues located in extracellular loop areas or close to them contribute to receptor selectivity. Moreover, recent molecular dynamics simulations of agonist binding to human TAS2R46 suggested the presence of a transient, vestibular ligand binding site that may contribute to ligand selectivity in addition to the orthosteric binding site [32]. For the TAS2R14, steric exclusion of agonists seems to represent a minor constraint, because additions of large side-chains, as long as one ligand dimension (dimension B, cf. Figs. 4 and 5) stays below ~ 7 Å, retained agonistic activity or even became more potent.

Furthermore, structural analysis suggests that improved activity of benzoin derivatives compared to benzoin relates to hydrophobic interactions in general, and π - π stacking with His94^{3.37} in particular. Since mefenamic acid benzyl ester exhibited a somewhat reduced potency compared to mefenamic acid, the interaction with Gln266^{7.39} is of importance.

In summary, the current work demonstrated that chemical modification of TAS2R14 agonists allows to probe the spatial capacity of the binding pocket: the receptor TAS2R14 is able to accommodate agonists with a wide range of sizes, as typical for multi-specific GPCRs [33], indicating that agonist-receptor contact points do not envelop the ligand tightly. This is in agreement with the finding that TAS2R promiscuity correlates with the binding site surface [34]. Future work elucidating the contact points between TAS2R14 binding site residues and its agonists is necessary to reveal the molecular basis for the promiscuity of this receptor aside from its apparent spacious ligand binding site.

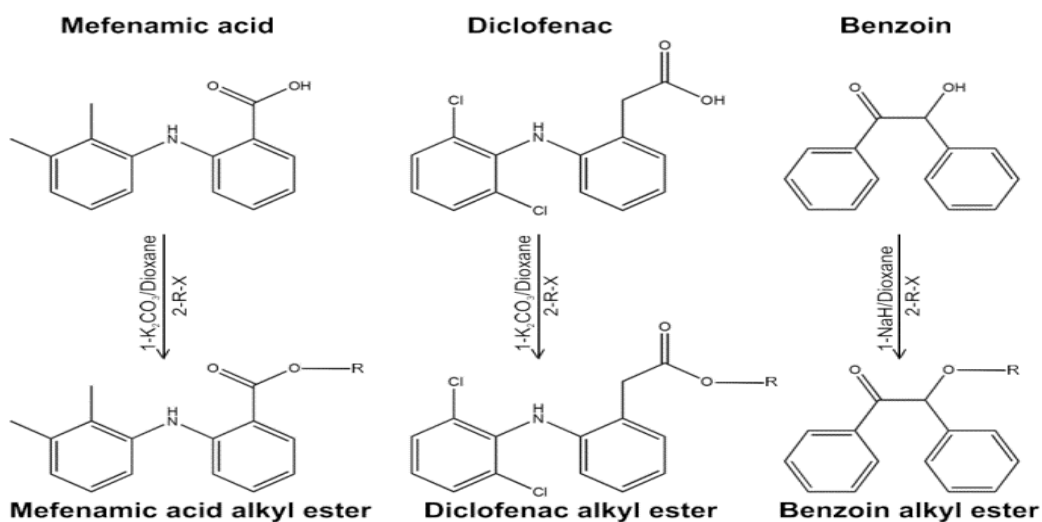


Figure (2): Chemical structures of the cognate TAS2R14 agonists and schematic representation of syntheses performed for chemical modifications. The chemical structures of the two anti-inflammatory drugs, mefenamic acid and diclofenac, and of the natural bitter substance benzoin are depicted. The synthesis strategies for mefenamic acid and diclofenac alkyl esters, mefenamic acid hexyl, mefenamic acid decyl, mefenamic acid benzyl, diclofenac hexyl and diclofenac benzyl esters as well as benzoin alkyl ethers, benzoin hexyl and benzoin benzyl ethers, respectively, are indicated. $R-X$ = Hexyl iodide, decyl iodide (only for mefenamic acid modification), benzyl bromide.

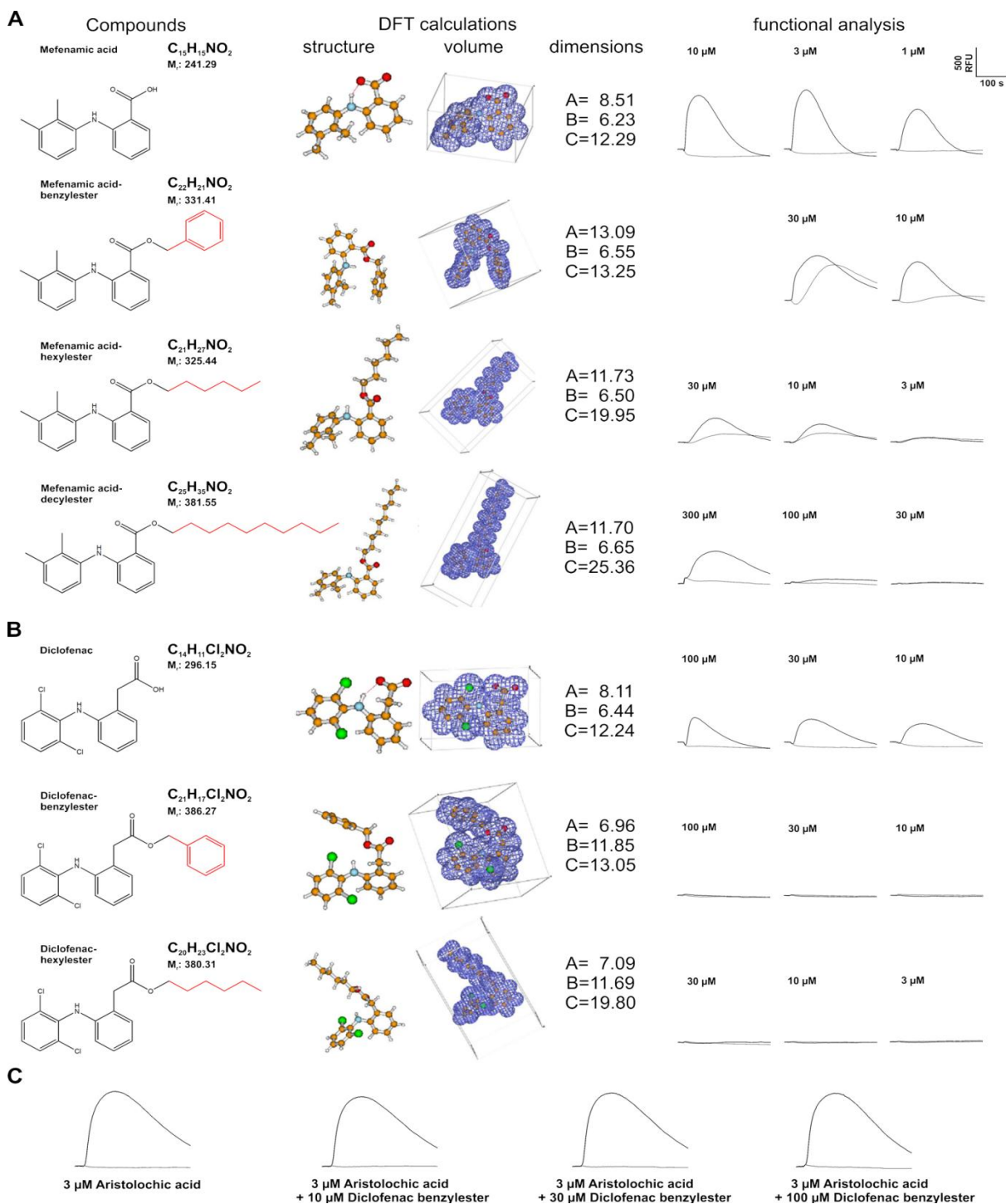


Figure (3): Chemical structures, DFT-calculated 3D-cell volumes, and receptor activating properties of mefenamic acid and diclofenac derivatives. Chemical structures of mefenamic acid (A) and diclofenac (B) derivatives are provided together with molecular formulas and the corresponding molecular weights. Side chains added to the original

agonists are highlighted in red. DFT optimized structures are shown in balls and sticks models, the calculated surface areas are illustrated, and the dimensions in Å are given. Changes in fluorescence after agonist application and applied agonist concentrations are shown on the right. Black traces were obtained from HEK 293T-Gα16gust44 cells transiently transfected with TAS2R14 cDNA, gray traces represent negative controls obtained by stimulation of cells transfected with empty expression vector. C) To investigate competition for the ligand binding site of TAS2R14 different mixtures of aristolochic acid and diclofenac benzyl ester were added to HEK 293T-Gα16gust44 cells transiently transfected with TAS2R14 cDNA and fluorescence changes were monitored. Note the stable amplitudes obtained for the agonist aristolochic acid alone and together with increasing concentrations of diclofenac benzyl ester. Black traces were obtained from HEK 293T-Gα16gust44 cells transiently transfected with TAS2R14 cDNA, gray traces represent negative controls obtained by stimulation of cells transfected with empty expression vector.

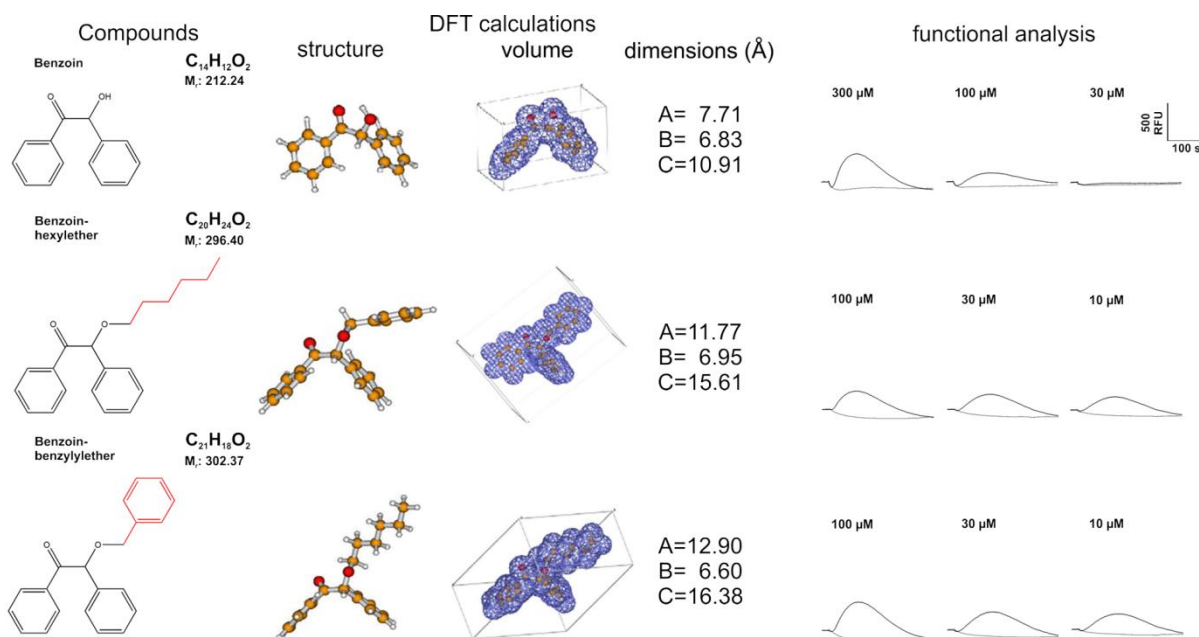


Figure (4): Chemical structures, DFT-calculated 3D-cell volumes, and receptor activating properties of benzoïn derivatives. Chemical structures of the specified compounds are provided together with molecular formulas and the corresponding molecular weights. Side chains added to the original agonists are highlighted in red. DFT optimized

structures are shown in balls and sticks models, the calculated surface areas are illustrated, and the dimensions in Å are given. Changes in fluorescence after agonist application and the applied agonist concentrations are shown on the right. Black traces were obtained from HEK 293T-Gα16gust44 cells transiently transfected with TAS2R14 cDNA, gray traces represent negative controls obtained by stimulation of cells transfected with empty expression vector. Note, that the addition of hydrophobic side chains to benzoin results in elevated potencies of the modified derivatives.

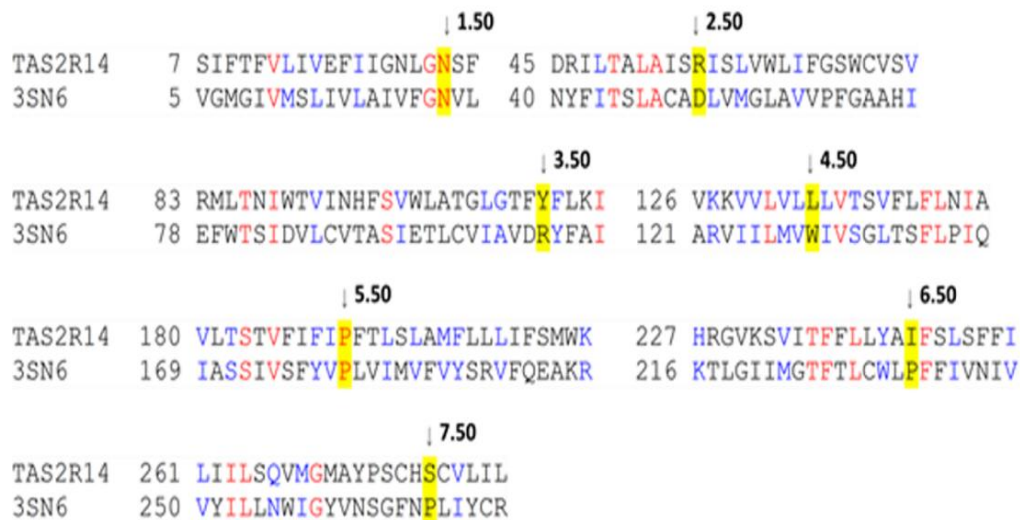


Figure (5): Sequence alignment of modeled TAS2R14 receptor and the template X-ray structure of β2 adrenergic receptor (PDB ID: 3SN6). Identical residues are shown in red and similar residues in blue. Positions X.50 according to the Ballesteros-Weinstein numbering system are shaded yellow.

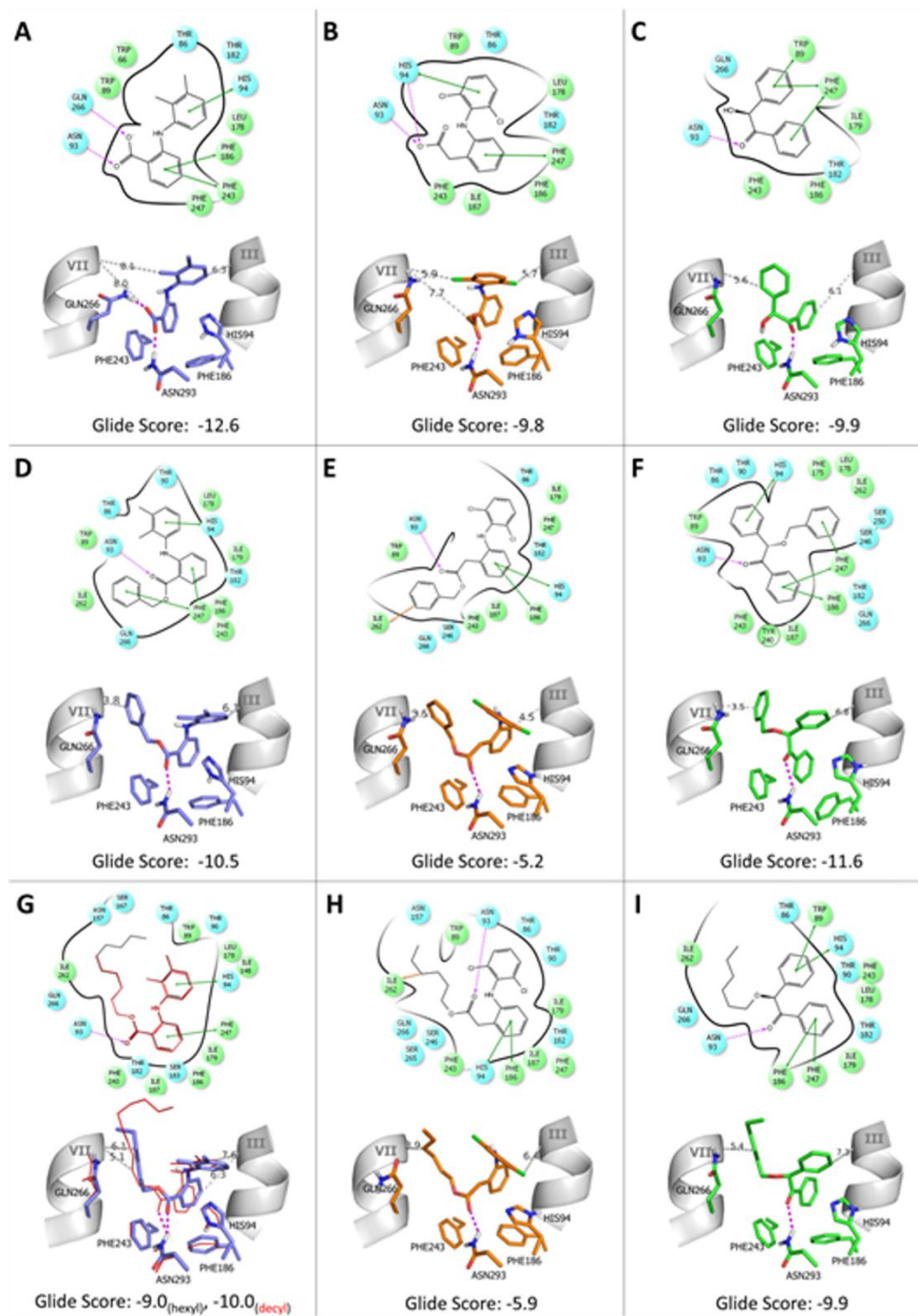
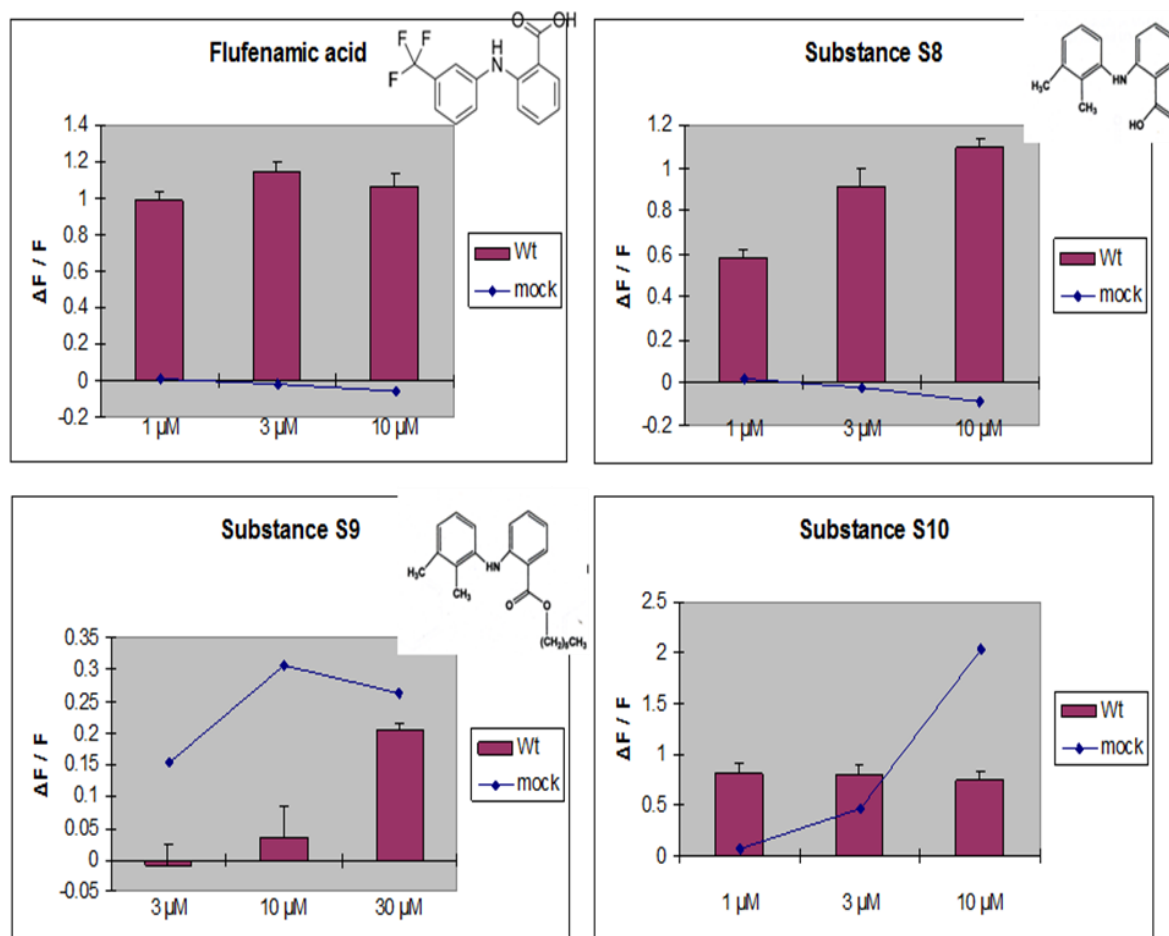


Figure (6): 3D and 2D representation of the docking pose of mefenamic acid (**A**), diclofenac (**B**), benzoin (**C**) and their derivatives (benzyl derivatives in **D**, **E** and **F**; hexyl derivatives in **G**, **H** and **I**) with TAS2R14 receptor. Mefenamic acid and its derivatives are shown in violet sticks (with the exception of mefenamic decyl ester represented in red

line, panel G), diclofenac and its derivatives in orange, benzoin and their derivatives in green. H-bond interactions are shown in magenta, π - π interactions in green and bad contacts are indicated by red arrows. In the 3D representations, only polar interactions are reported, and the distance between the ligands and C- α of the residues Ile179^{5,39} and Ile262^{7,35} are reported in dashed gray lines. In 2D representations, polar and hydrophobic residues are shown as cyan and green spheres, respectively.

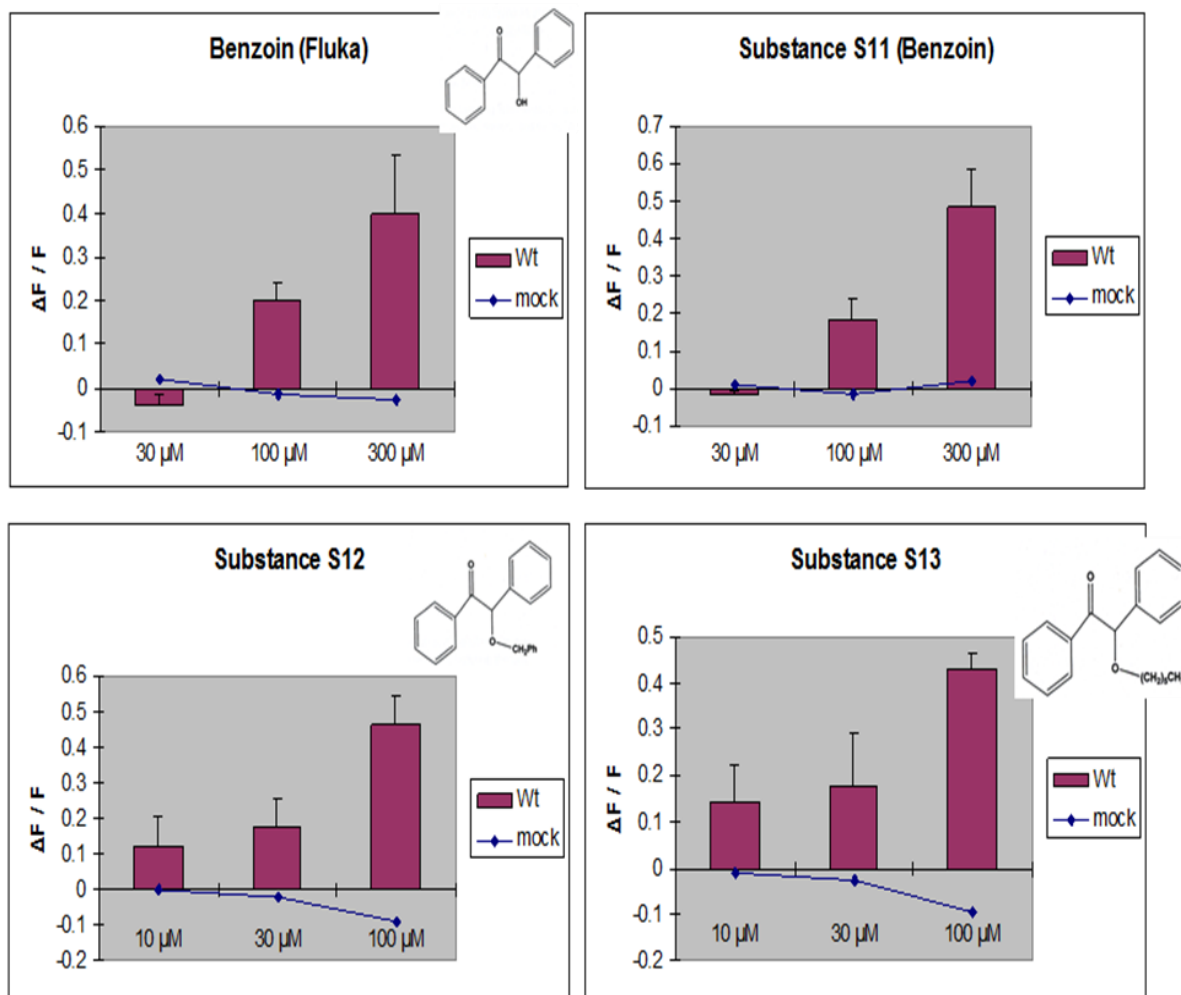
The mefenamic acid (S8) standard shows in the graph bitterness at 1,3,10 micro molar, but we observed by combining iodohexane to mefenamic (S9) less bitterness more than 10 fold than bezyl mefenamate (S10) were observed (Fig. 7)

For benzoin (S11) the bitterness can be observed at 100, 300 micro molar, the bitterness became more agonist for benzyl benoinat (S12) and so hexyl benoinat (S13) (Fig.8)



Stefanie Nowak, 04.10.2012

Figure (7). The mefenamic acid (S8) standard shows in the graph bitterness at 1,3,10 micro molar, but we observed by combining iodohexane to mefenamic (S9) less bitterness than bezyl mefenamate (S10) were observed.



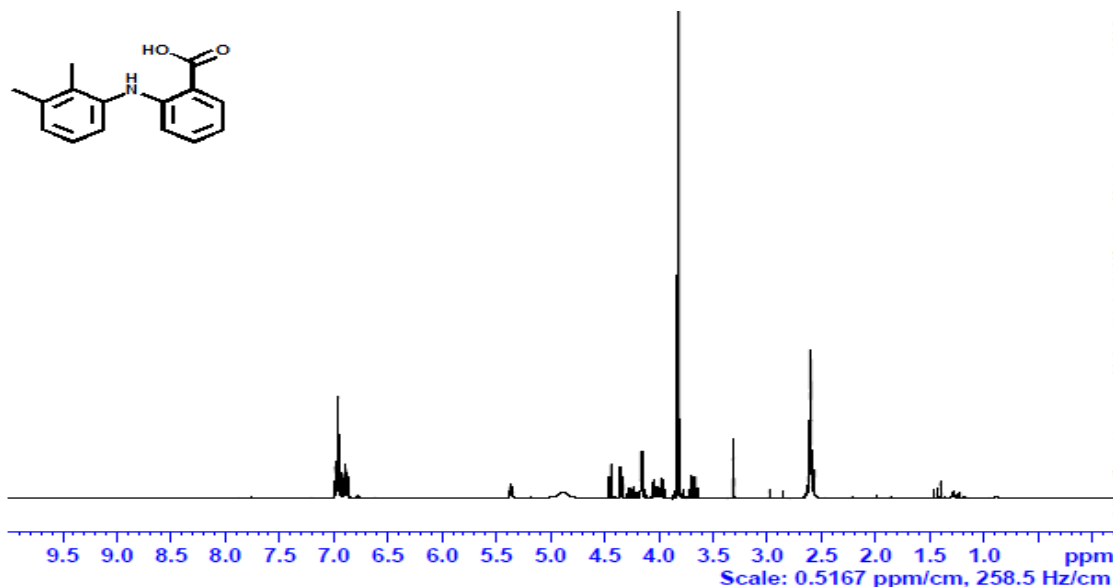
Stefanie Nowak, 04.10.2012

Figure (8). For benzoin (S11) the bitterness can be observed at 100, 300 micro molar, the bitterness became more agonist for benzyl benoinat (S12) and so hexyl benzoinat (S13)

4.2.2 Analytical data for the synthesized organic compounds

4.2.2.1 Mefenamic Acid-

Appearance (Fig. 13): yellowish crystals M.P. 230-231 °C. $^1\text{H-NMR}$ δ (ppm) CD 3 OD :2.16 (s, 3H, Ar-(CH₃)) , 2.35 (s , 3H, Ar-(CH₃)) , 6.63 (t, 1H, Ar-H), 7.01(d, 2H, J=6.7 ,Ar-H), 7.11 (t, 1H, Ar-H), 7.23 (t, 1H, Ar-H), 7.94 (d, 2H, J=1.65, Ar-H).



Figure(9) $^1\text{H-NMR}$ spectrum of mefenamic acid in CD₃OD S8

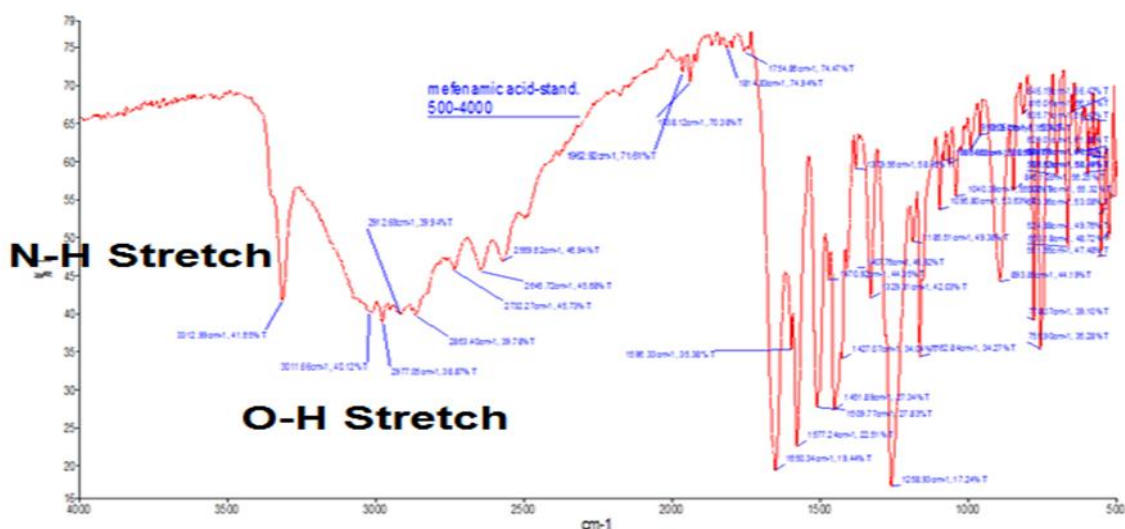


Figure (10): IR result of mefenamic acid

4.2.2.2 Mefenamic hexyl ester –

Appearance (Fig. 10): yellowish oil. $^1\text{H-NMR}$ δ (ppm) CDCl_3 - 0.87 (t, 3H, $J=6.8$ Hz, CH_2CH_3), 1.35-1.47 (m, 6H, $\text{CH}_2\text{CH}_2\text{CH}_2\text{CH}_3$), 1.62 (m, 2H, $\text{OCH}_2\text{CH}_2\text{CH}_2$), 2.18 (s, 3H, Ar- CH_3), 2.32 (s, 3H, Ar- CH_3), 4.30 (t, 2H, $J=7.6$ Hz, OCH_2), 6.65 (d, 1H, $J=8$ Hz, Ar-H), 7.01 (m, 2H, Ar-H), 7.10 (m, 2H, Ar-H), 7.24 (dt, 1H, $J=14$ Hz, Ar-H), 7.95 (dd, 1H, $J=8$ Hz, Ar-H). IR ($\text{KBr}/\nu_{\text{max}}$ cm^{-1}) 3318 (NH), 2910 (alkyl), 1685 ($\text{C}=\text{O}$), 1607 ($\text{C}=\text{C}$), 1249 ($\text{C}-\text{O}$), 1160 ($\text{C}-\text{O}$) 1085 ($\text{C}-\text{O}$). m/z 326.2853 ($\text{M}+1$) $^+$.

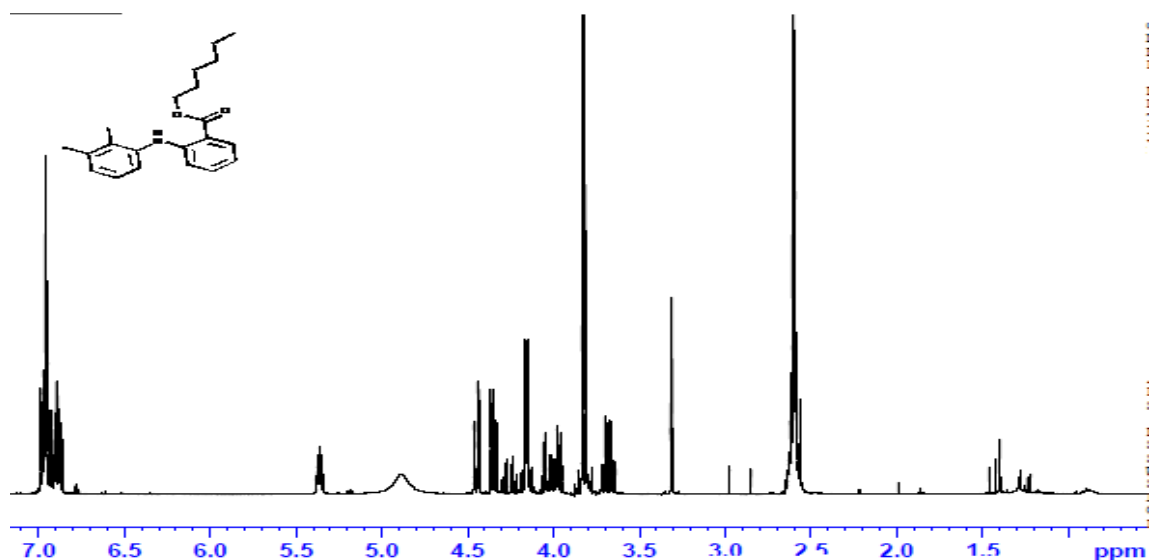


Figure (11) $^1\text{H-NMR}$ spectrum of mefenamic hexyl in CD_3OD S9

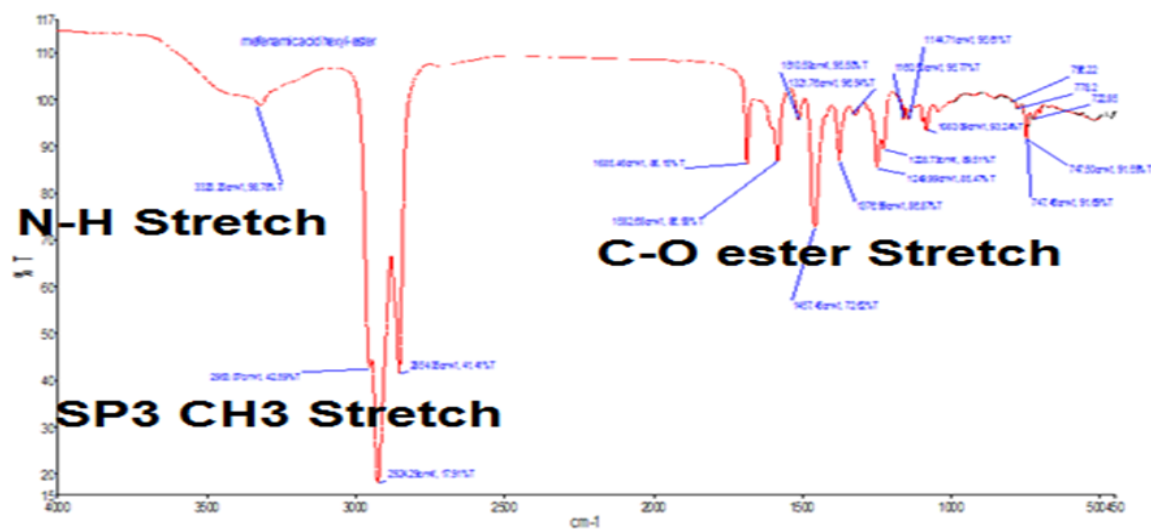


Figure (12) IR spectrum of mefenamic hexyl S9

4.2.2.3 Mefenamic benzyl ester

Appearance (Fig. 9): yellowish crystals M.P. 107-110 °C. $^1\text{H-NMR}$ δ (ppm) CDCl_3 - 2.18 (s, 3H, Ar-CH3), 2.32(s, 3H, Ar-CH3), 4.91 (s, 2H, OCH2), 6.68 (m, 2H, Ar-H), 6.90 (m, 2H, Ar-H), 7.06 (m, 1H, Ar-H), 7.22 (m, 1H, Ar-H), 7.31 (m, 1H, Ar-H), 7.45 (m, 6H, Ar-H), 7.97 (dd, 1H, J=8 Hz, Ar-H). IR (KBr/ ν_{max} cm^{-1}) 3318 (NH), 2910 (alkyl), 1726 (C=O), 1607 (C=C), 1249 (C-O), 1160 (C-O) 1085 (C-O). m/z 332.2653 (M+1) $^+$.

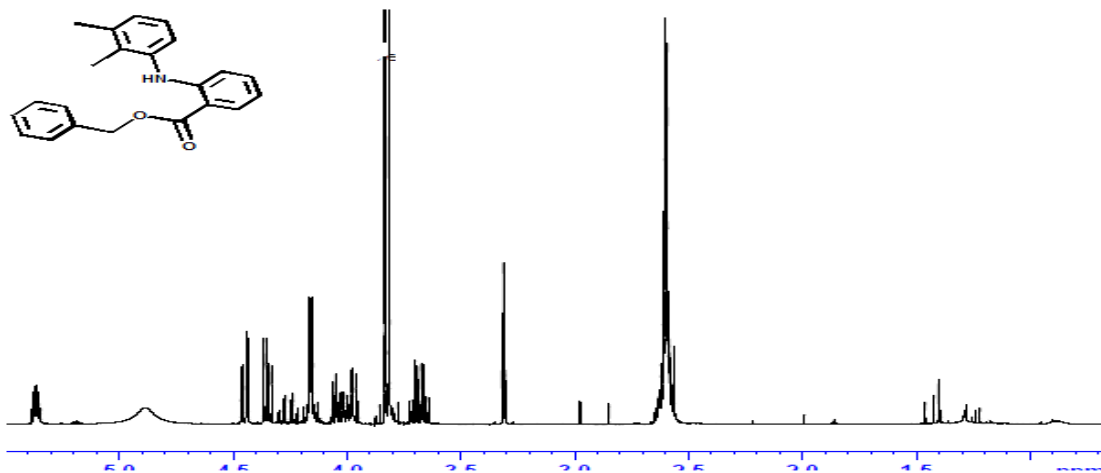


Figure (13) $^1\text{H-NMR}$ spectrum of mefenamic benzyl in CD_3OD S10

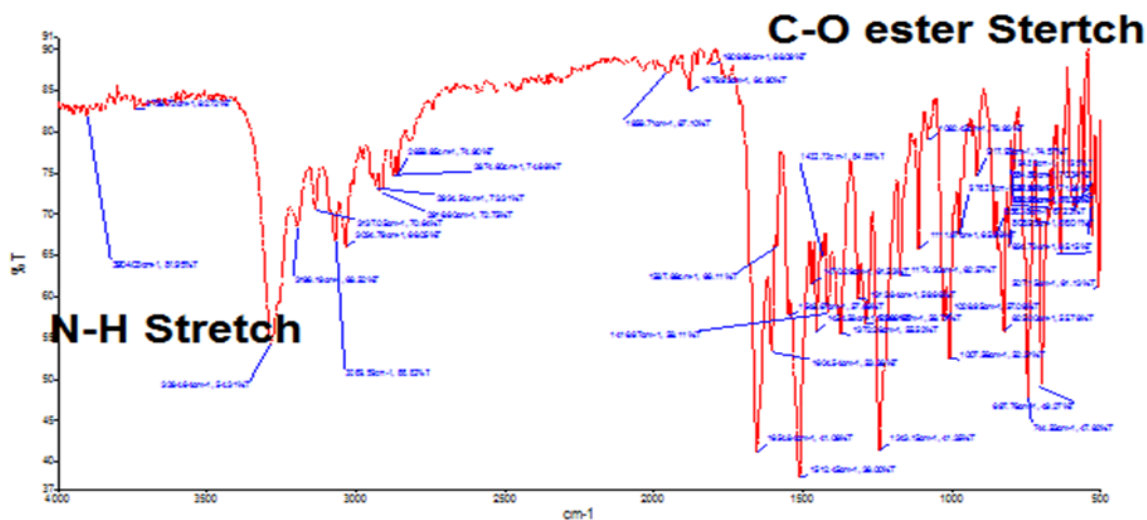


Figure (14) IR spectrum of mefenamic benzyl S10

4.2.2.4 Mefenamic decyl ester –

Appearance (FNS): yellowish oil. $^1\text{H-NMR}$ δ (ppm) CDCl_3 - 0.87 (t, 3H, $J=6.8$ Hz, CH_2CH_3), 1.34-1.57 (m, 14H, $(\text{CH}_2)_7\text{CH}_3$), 1.51 (m, 2H, $\text{OCH}_2\text{CH}_2\text{CH}_2$), 2.20 (s, 3H, Ar- CH_3), 2.28 (s, 3H, Ar- CH_3), 4.33 (t, 2H, $J=7.6$ Hz, OCH_2), 6.67 (d, 1H, $J=8$ Hz, Ar-H), 7.04 (m, 2H, Ar-H), 7.12 (m, 2H, Ar-H), 7.24 (dt, 1H, $J=14$ Hz, Ar-H), 7.98 (dd, 1H, $J=8$ Hz, Ar-H). IR (KBr/ ν_{max} cm^{-1}) 3325 (NH), 2925 (alkyl), 1682 (C=O), 1597 (C=C), 1259 (C-O), 1163 (C-O) 1075 (C-O). m/z 382.2723 ($\text{M}+1$) $^+$.

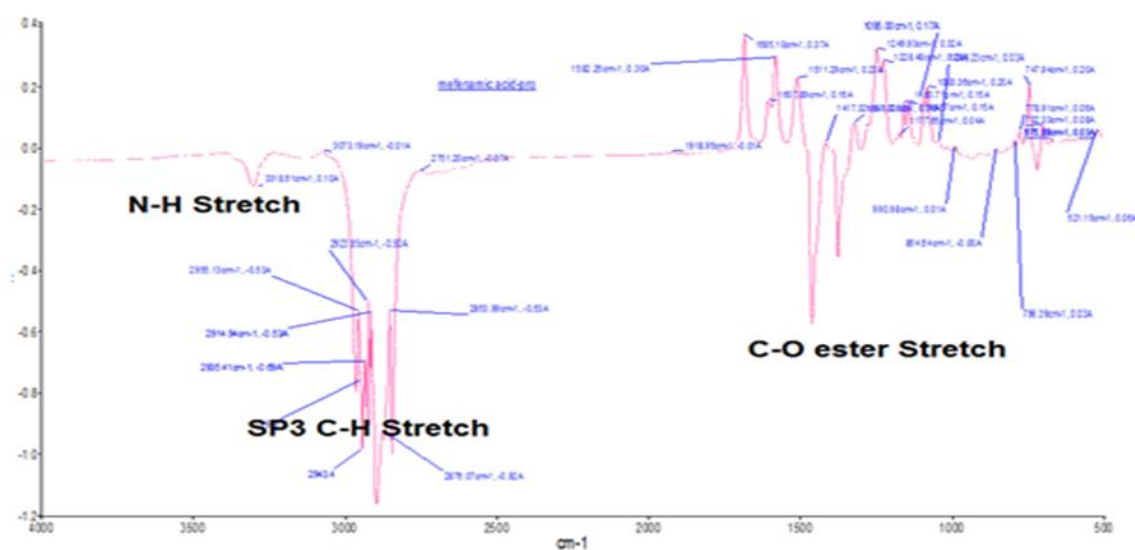


Figure (15) IR spectrum of mefenamic decyl

4.2.2.5 Diclofenac (from Ala Thesis NMR & et..)

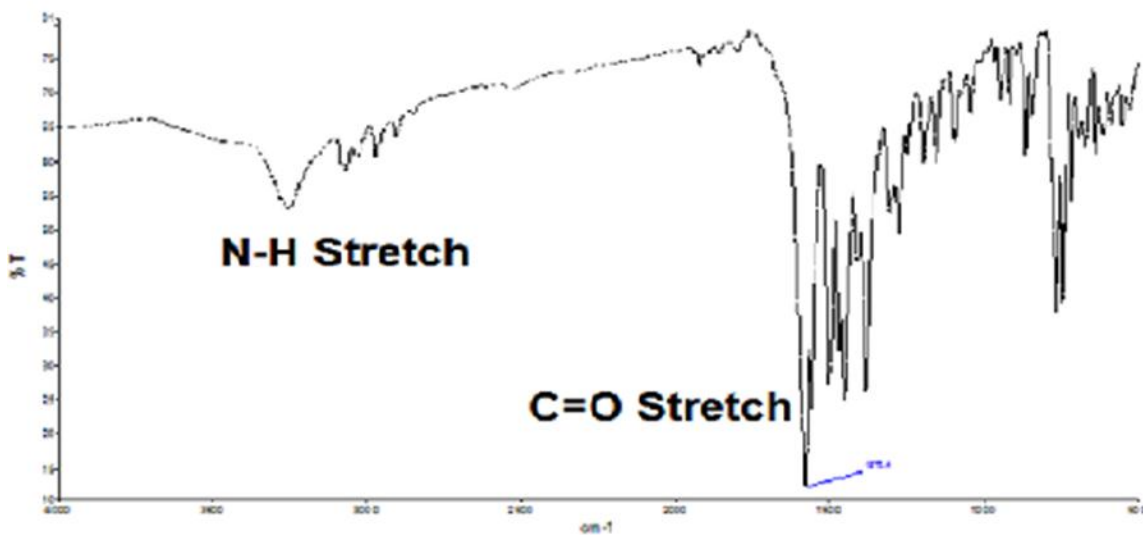


Figure (16) IR spectrum of Diclofenac

4.2.2.6 Diclofenac hexyl ester –

Appearance (FNS): Brownish oil. ¹H-NMR δ (ppm) CDCl₃- 0.86 (t, 3H, J=6.8 Hz, CH₂CH₃), 1.24-1.30 (m, 6H, CH₂CH₂CH₂CH₃), 1.63(m, 2H, OCH₂CH₂CH₂), 3.86 (s, 2H, COCH₂), 4.12 (t, 2H, J=7.6 Hz, OCH₂), 6.53 (d, 1H, J= 8 Hz, Ar-H), 6.93 (d, 1H, J= 21.6 Hz, CH₂-Ar-H), 6.95 (t, 1H, Ar-H), 7.14 (t, 1H, Ar-H), 7.24 (d, 1H, J=1.6 Hz , Ar-H), 7.32 (m , 2H, Ar-H). IR (KBr/ ν_{\max} cm⁻¹) 3361 (NH), 2955 (alkyl), 1714 (C=O), 1590 (C=C), 1283 (C-O), 1117 (C-O), 1081 (C-O). *m/z* 381.1183 (M+1)⁺.

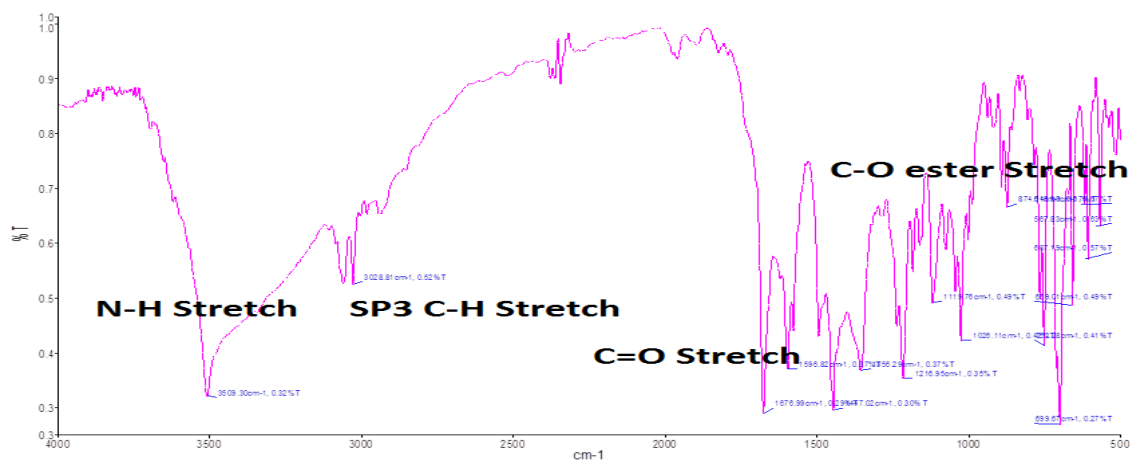


Figure (17) IR spectrum of Diclofenac hexyl ester

4.2.2.7 Diclofenac benzyl ester –

Appearance (FNS): white crystals, M.P. > 300 °C (not corrected). $^1\text{H-NMR}$ δ (ppm) CDCl_3 - 3.86 (s, 2H, COCH_2), 5.12 (s, 2H, CH_2 -Ar), 6.54 (d, 1H, $J=8$ Hz, Ar-H), 6.88 (d, 2H, $J=21.6$ Hz, CH_2 -Ar-H), 6.97 (t, 1H, Ar-H), 7.14 (t, 1H, Ar-H), 7.24 (d, 1H, $J=1.6$ Hz, Ar-H), 7.31 (d, 1H, $J=3.2$ Hz, Ar-H), 7.33 (t, 5H, Ar-H). IR ($\text{KBr}/v_{\text{max}}$ cm^{-1}) 3361 (NH), 1743 (C=O), 1588 (C=C), 1576 (C=C), 1563 (C=C), 1557 (C=C), 1283 (C-O), 1178 (C-O), 1091 (C-O). m/z 387.0710 ($\text{M}+1$) $^+$.

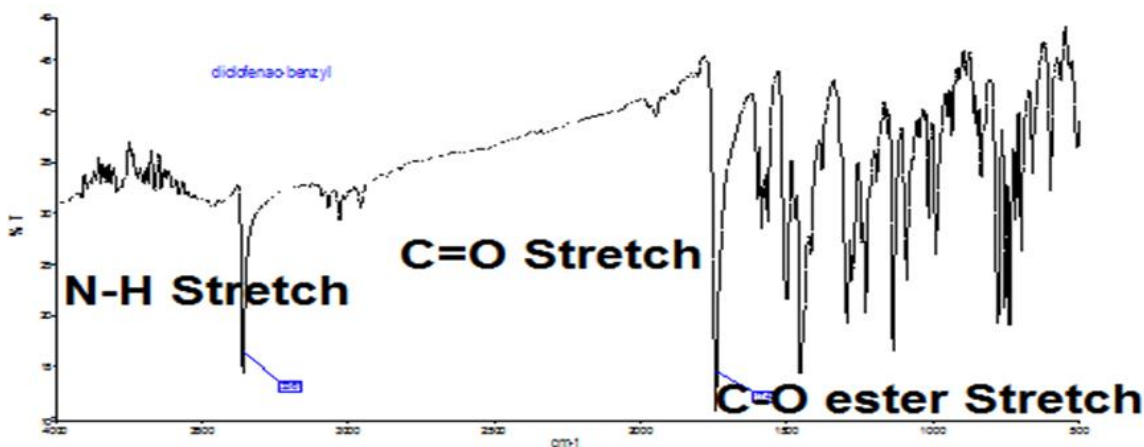


Figure (18) IR spectrum of Diclofenac benzyl ester

4.2.2.8 benzoin (

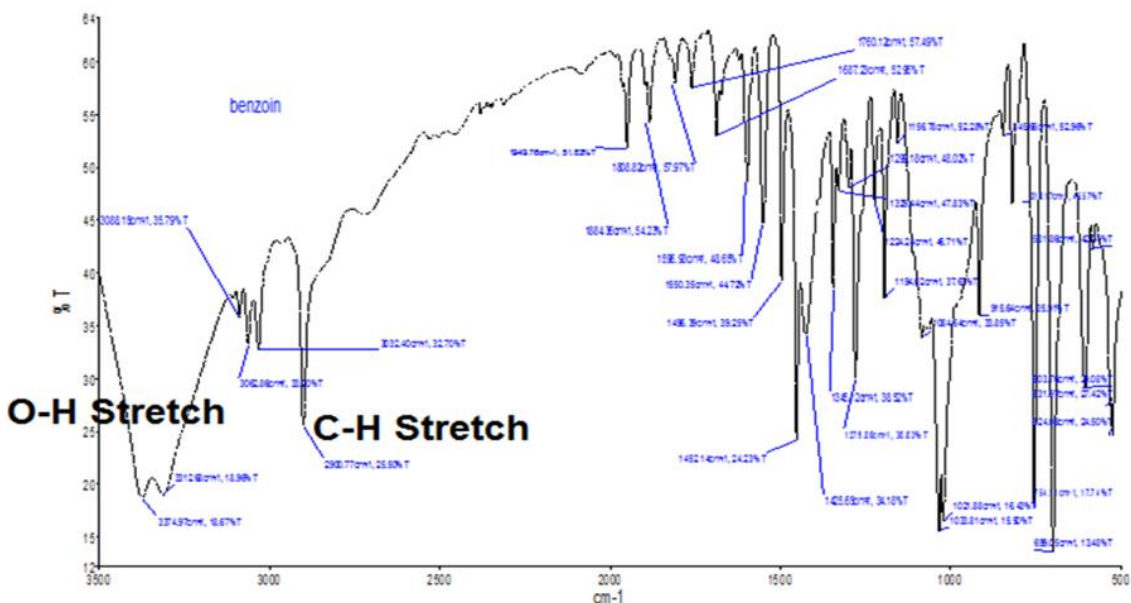


Figure (19) IR spectrum of benzoin

4.2.2.9 Benzoin hexyl ether –

Appearance (Fig. 12): yellowish crystals M.P. 80-82 °C (not corrected). $^1\text{H-NMR}$ δ (ppm) CDCl_3 - 0.88 (t, 3H, $J=6.8$ Hz, CH_2CH_3), 1.21-1.51 (m, 6H, $\text{CH}_2\text{CH}_2\text{CH}_2\text{CH}_3$), 1.62 (m, 2H, $\text{OCH}_2\text{CH}_2\text{CH}_2$), 3.88 (t, 2H, $J=7.6$ Hz, OCH_2), 6.63 (d, 1H, $J=8$ Hz, Ar-H), 7.33 (m, 3H, Ar-H), 7.61 (m, 4H, Ar-H), 8.05 (dd, 2H, $J=8$ Hz, Ar-H). IR (KBr/ ν_{max} cm^{-1}) 3318 (NH), 2910 (alkyl), 1685 (C=O), 1607 (C=C), 1249 (C-O), 1160 (C-O) 1085 (C-O). 297.1809 ($\text{M}+1$) $^+$.

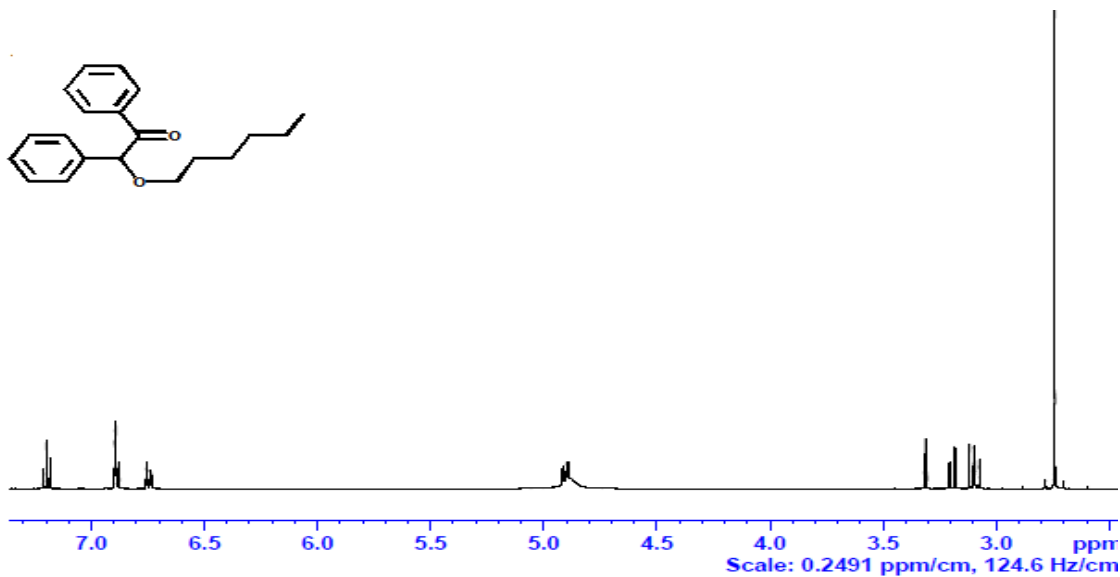


Figure (20) $^1\text{H-NMR}$ spectrum of benzoin hexyl in CDCl_3

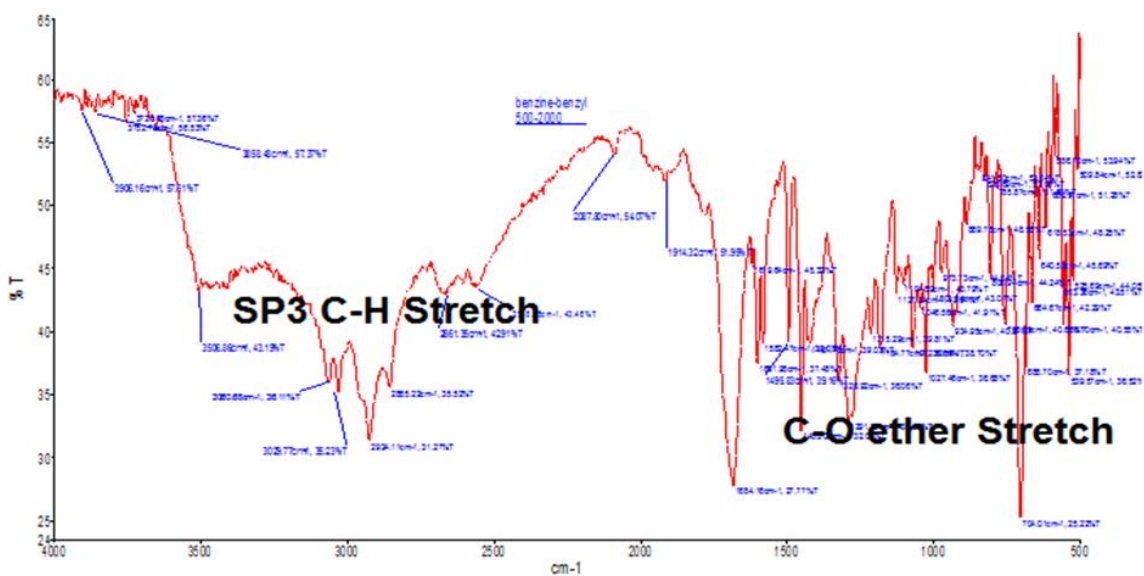


Figure (21) IR spectrum of benzoin hexyl

4.2.2.10 Benzoin benzyl ether –

Appearance (Fig. 11): yellowish crystals M.P. 110-112 °C (not corrected). $^1\text{H-NMR}$ δ (ppm) CDCl_3 - 4.41 (s, 2H, $\text{O-CH}_2\text{Ph}$), 6.61(s, 1H, $\text{CHO-CH}_2\text{Ph}$), 7.32 (m, 5H, Ar-H), 7.36 (m, 2H, Ar-H), 7.38 (m, 3H, Ar-H), 7.64 (m, 3H, Ar-H), 7.94 (dd , 2H, $J=8$ Hz, Ar-

H). IR (KBr/ ν_{\max} cm^{-1}) 1686 (C=O), 1607 (C=C), 1249 (C-O), 1160 (C-O) 1085 (C-O).
 m/z 303.1380 (M+1)⁺.

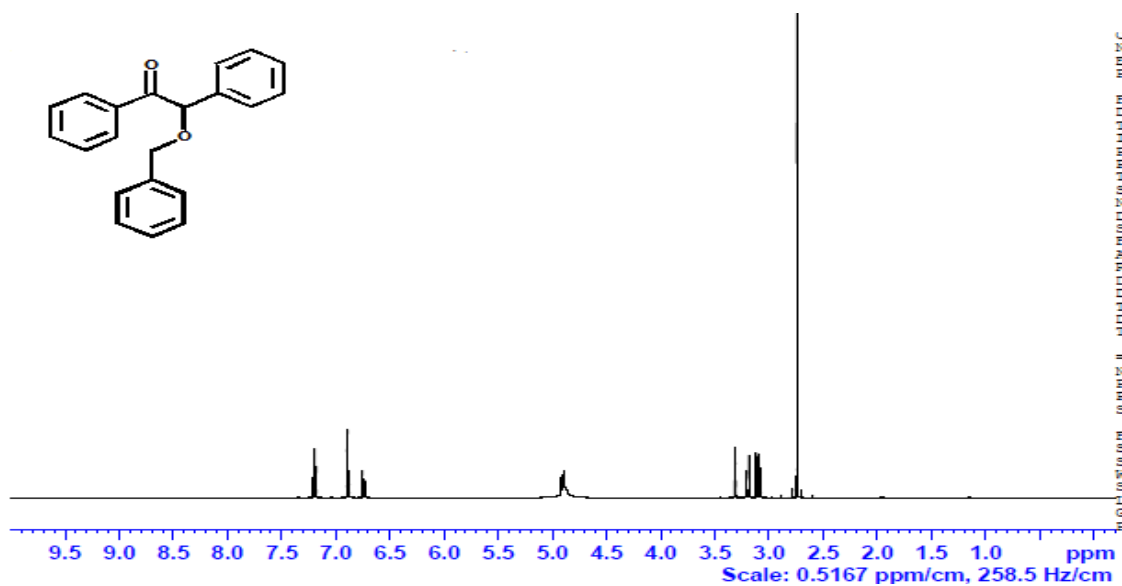


Figure (20) ¹H-NMR spectrum of benzoin benzyl in CDCl₃

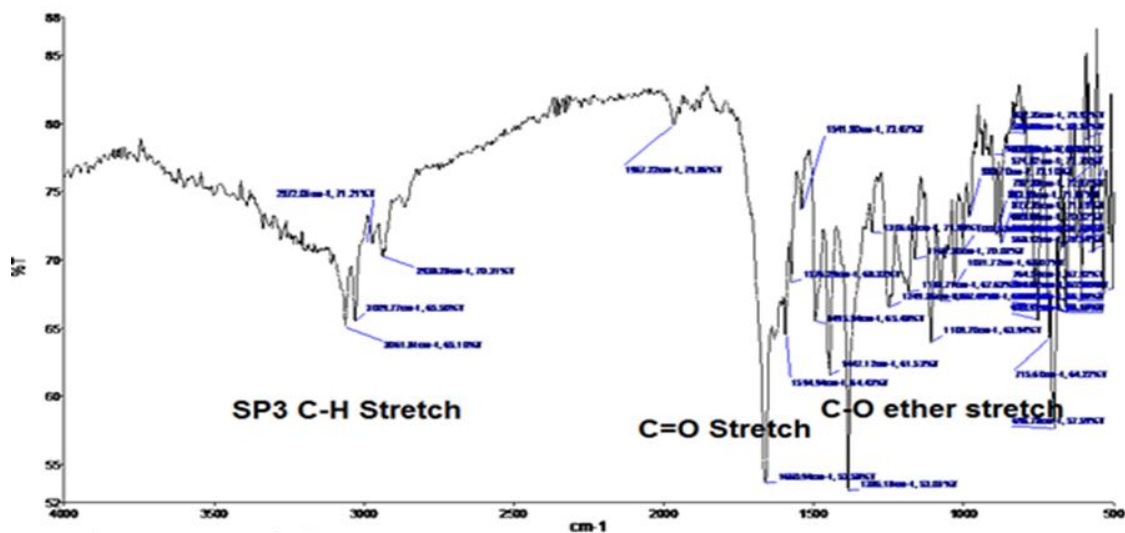


Figure (22) IR spectrum of benzoin benzyl

Table 2: Glide XP scores for mefenamic acid, diclofenac, benzoin and their derivatives in complex with TAS2R14 structure.

Ligand	Glide XP Score (kcal/mol)
Mefenamic acid	-12.6
Mefenamic benzyl ester	-10.5
Mefenamic hexyl ester	-9.0
Mefenamic decyl ester	-10.0
Diclofenac	-9.9
Diclofenac benzyl ester	-5.2
Diclofenac hexyl ester	-5.9
Benzoin	-9.8
Benzoin benzyl ether	-11.6
Benzoin hexyl ether	-9.9

Summary:

In summary, the current work demonstrated that chemical modification of TAS2R14 agonists allows to probe the spatial capacity of the binding pocket: the receptor TAS2R14 is able to accommodate agonists with a wide range of sizes, as typical for multispecific GPCRs, indicating that agonist-receptor contact points do not envelop the ligand tightly. This is in agreement with the finding that TAS2R promiscuity correlates with the binding site surface. Future work elucidating the contact points between TAS2R14 binding site residues and its agonists is necessary to reveal the molecular basis for the promiscuity of this receptor aside from its apparent spacious ligand binding site.

References:

1. Sohi H, Sultana Y, Khar RK. Taste Masking Technologies in oral pharmaceuticals, recent development and approaches. *Drug Develop. Ind. Pharm.* 2004;30(5): 429-448.
2. Reilly WJ. *Pharmaceutical necessities in Remington: The science and practice of pharmacy*, Mack Publishing Company; 2002. p 1018-1020.
3. Gowan Jr. WG, Richard DB. Aliphatic esters as a solventless coating for pharmaceuticals. No. CA2082137. 19 Aug. 2003.
4. Gowthamarajan K, Kulkarni G T, Kumar MN. Pop the pills without bitterness. *Resonance* 2004;9(12): 25-32.
5. Davis JD. *Drug Cosmet. India: Encyclopedia of pharmaceutical technology.* 2000;2: 1-5.
6. Bakan JA. *Microencapsulation, Theory and practice of Industrial Pharmacy*, Third Edition 1986. p 412-429.
7. Ikeda K. New seasonings. *Chemical senses* 2002;27(9): 847-849.
8. Maehashi K, Matano M, Wang H, Vo LA, Yamamoto Y, Huang L. Bitter peptides activate hTAS2Rs, the human bitter receptors. *Biochemical and biophysical research communications* 2008;365(4): 851-855.
9. Lindemann B. Receptors and transduction in taste. *Nature* 2001;413(6852): 219-225.
10. Behrens M, Meyerhof W. Bitter taste receptors and human bitter taste perception. *Cell Mol. Life Sci.* 2006;63: 1501–1509.
11. Meyerhof W, Born S, Brockhoff A, Behrens M. Molecular biology of mammalian bitter taste receptors. A review. *Flavour Frag. J.* 2011;26: 260–268.

12. Behrens M, Meyerhof W. Mammalian bitter taste perception. *Results Probl. Cell. Differ.* 2009;47: 203–220.
13. Brockhoff A, Behrens M, Massarotti A, Appendino G, Meyerhof W. Broad tuning of the human bitter taste receptor hTAS2R46 to various sesquiterpene lactones, clerodane and labdane diterpenoids, strychnine, and denatonium. *J. Agric. Food Chem.* 2007;55: 6236–6243.
14. Meyerhof W, Batram C, Kuhn C, Brockhoff A, Chudoba E, Bufe B, Appendino G, Behrens M. The molecular receptive ranges of human TAS2R bitter taste receptors. *Chem. Senses* 2010;35: 157–170.
15. Wiener A, Shudler M, Levit A, Niv MY. Bitter DB: a database of bitter compounds. *Nucleic acids research* 2012;40(D1): D413-D419.
16. Bufe B, Hofmann T, Krautwurst D, Raguse JD, Meyerhof W. The human TAS2R16 receptor mediates bitter taste in response to beta-glucopyranosides. *Nat. Genet.* 2002;32: 397–401.
17. Sainz E, Cavenagh MM, Gutierrez J, Battey JF, Northup JK, Sullivan SL. Functional characterization of human bitter taste receptors. *Biochem. J.* 2007;403: 537–543.
18. Sakurai T, Misaka T, Ishiguro M, Masuda K, Sugawara T, Ito K, Kobayashi T, Matsuo S, Ishimaru Y, Asakura T. et al. Characterization of the beta-D-glucopyranoside binding site of the human bitter taste receptor hTAS2R16. *J. Biol. Chem.* 2010; 285: 28373–28378.
19. Hunter G, Wayne ED, Timothy DN, Peter S, Alicia E, Gary G. Pseudoephedrine is without ergogenic effects during prolonged exercise. *Journal of Applied Physiology* 1996;81: 2611–2617.
20. Malladi M, Jukanti R, Nair R, Wagh S, Padakanti H, Matet A. Design and Evaluation of Taste Masked Dextromethorphan Hydrobromide Oral Disintegrating Tablets. *Acta Pharmaceutica* 2010; 60: 267–280.

21. Schwabe U, Ukena D, Lohse MJ. Xanthine derivatives as antagonists at A1 and A2 adenosine receptors. *Naunyn-Schmiedeberg's Archives of Pharmacology* 1985;330(3): 212–21.
22. Mycek MJ, Harvey RA, Champe RC. *Lippincott's illustrated reviews pharmacology*. Philadelphia: Lippincott-Raven; 1997.
23. Grover R, Frank ME. Regional Specificity of Chlorhexidine Effects on Taste Perception; *Chem Senses* 2008; 33(4): 311-318.
24. Stokbroekx RA, Vanenberk J, Van Heertum AHMT, Van Laar GMLW, Van der Aa MJMC, Van Bever WFM, Janssen PAJ. Synthetic Antidiarrheal Agents. 2,2-Diphenyl-4-(4'-aryl-4'-hydroxypiperidino)butyramides. *Journal of Medicinal Chemistry* 1973; 16(7): 782–786.
25. Thompson D, Oster G. Use of Terfenadine and Contraindicated Drugs. *Journal of the American Medical Association (American Medical Association)* 1996; 275 (17): 1339–1341.
26. Rossi S. *Australian Medicines Handbook*. AMH.ISBN 2004; 0-9578521-4-2.
27. Karaman R. Computationally Designed Prodrugs for Masking the Bitter Taste of Drugs. *Journal of Drug Designing* 2012;1:e106. doi:10.4172/2169-0138.1000e106.
28. Karaman R. “A Solution to Aversive Tasting Drugs for Pediatric and Geriatric Patients” *Journal of Drug Designing , Drug Des.* 2013;DOI:10.4172/2169-0138.1000e116.
29. Karaman R. “The Future of Prodrugs designed by Computational Chemistry” *Journal of Drug Designing*, 2012; 1:e103. doi:10.4172/ddo.1000e103.
30. Ayenew Z, Puri V, Kumar L, Bansal AK. Trends in Pharmaceutical Taste Masking Technologies: A Patent Review. *Recent Patents on Drug Delivery & Formulation* 2009;3: 26-39.

31. Fawzy AA. Pleasant Tasting Aqueous Liquid Composition of a Bitter-Tasting Drug, PCT Int. Appl. 1998; WO9805312, 2.
32. Zelalem A, Puri V, Kumar L, Bansal A. Trends in Pharmaceutical Taste Masking Technologies: A Patent Review. Recent Patents on Drug Delivery & Formulation 2009;3, 26-39.
33. Jain NK. Advances in controlled and Novel Drug delivery 2001; 1stEd, 290-306.
34. Bress WS, Kulkarni N, Ambike S, Ramsay MP. 2006; EP1674078.
35. Mendes WR. Theory and practice of Industrial pharmacy, Third Edition; 1976.
36. Redondo AMJ, Abanades LB. 2003; WO047550.
37. Kashid N, Chouhan P, Mukherji G. 2007; WO2007108010.
38. Burgard A. 2003; JP026665.
39. Lachman L, Liberman HA. Pharmaceutical Dosage Forms:Tablet”, Volume I; 1989,p 11-14.
40. Rao MY, Bader F. Masking the taste of chloroquine by Multiple Emulsion. The East. Pharm. 1993;123: 11.
41. Kasturagi Y. Selective inhibition of bitter taste of various drugs by lipoprotein.Pharm. Res. 1995;12(5): 658-662.
42. Brahmanekar DM., Jaiswal SB. Biopharmaceutics & Pharmaceutics. First Edition; 1995;pp 162-163.
43. Rozin, P., Vollmecke, T.A. Food Likes and Dislikes. Annu Rev Nutr. 1986; 6: 433-456.
44. Behrens, M., Meyerhof, W. Bitter taste receptor research comes of age: from characterization to modulation of TAS2Rs. Semin Cell Dev Biol. 2013 ;24: 215-221.

45. Meyerhof, W., Batram, C., Kuhn, C., Brockhoff, A., Chudoba, E., Bufe, B., Appendino, G., Behrens, M. The molecular receptive ranges of human TAS2R bitter taste receptors. *Chem Senses* 2010;35: 157-170.
46. Brockhoff, A., Behrens, M., Niv, M.Y., Meyerhof, W. Structural requirements of bitter taste receptor activation. *Proc Natl Acad Sci U S A.* 2010;107: 11110-11115.
47. Behrens, M., Brockhoff, A., Kuhn, C., Bufe, B., Winnig, M., Meyerhof, W. The human taste receptor hTAS2R14 responds to a variety of different bitter compounds. *Biochem Biophys Res Commun* 2004;319: 479-485.
48. Levit, A., Nowak, S., Peters, M., Wiener, A., Meyerhof, W., Behrens, M., Niv, M.Y. The bitter pill: clinical drugs that activate the human bitter taste receptor TAS2R14. *FASEB.* 2014; J;28: 1181-1197.
49. Foster, S.R., Blank, K., See Hoe, L.E., Behrens, M., Meyerhof, W., Peart, J.N., Thomas, W.G. Bitter taste receptor agonists elicit G-protein-dependent negative inotropy in the murine heart. *FASEB.* 2014; J;28: 4497-4508.
50. Karaman, R. Prodrugs for masking bitter taste of antibacterial drugs--a computational approach. *J Mol Model.* 2013;19: 2399-2412.
51. Aditi Tripathi, Dipika Parmar, Dr. Upendra Patel, Ghanshyam Patel, Dhiren Daslaniya, Bhavin Bhiman. Taste Masking: A Novel Approach for Bitter and Obnoxious Drugs 2011; *JPSBR*: 136-142
52. Shagufta Khan, Prashant Kataria, Premchand Nakhat. Taste masking of ondansetron hydrochloride by polymer carrier system and formulation of rapid-disintegrating tablets 2007; pp E127-E133.
53. Dev, S., Mhaske, D. V., Kadam, S. S., & Dhaneshwar, S. R. Synthesis and pharmacological evaluation of cyclodextrin conjugate prodrug of mefenamic acid. *Indian journal of pharmaceutical sciences* 2007; 69(1): 69.
54. Al-Omarn MF., Al-Suwayeh SA., El-Helw AM. And Saleh SI. Taste masking of diclofenac sodium using microencapsulation 2002; 19(1); 45-52.

55. Sona. P. S., Muthalingam C. Formulation and Evaluation of Taste Masked Orally Disintegrating Tablets of Diclofenac Sodium. International Journal of PharmTech Research. 2011;Vol.3, No.2, pp 819-826

تصنيع وتفعيل طعم المر لمستقبلات 14 (TAS2R14) - نهج لتعيين موقعها النشط

إعداد الطالب: حذيفة رشدي كتانه

المشرف الرئيسي: بروفيسور رفيق قرمان

ملخص:

الاستشعار عن المواد المريرة يمكن أن تكون ضارة في تجويف الفم ويتحقق من قبل مجموعة من ~ 25 المستقبلات، اسمه TAS2Rs، التي يتم التعبير عنها في الخلايا الحسية المتخصصة والتعرف على مجموعات فردية ولكن تداخل المركبات المريرة. المستقبلات تختلف في breadths ضبط والتي تتراوح من مستقبلات بصعوبة إلى ضبطها على نطاق واسع. واحد من مستقبلات الطعم المر الإنسان ضبطها أكثر على نطاق واسع هو TAS2R14 الاعتراف مجموعة متنوعة هائلة من الاصطناعية المتنوعة كيميائيا والمركبات المريرة الطبيعية، بما في ذلك العديد من العقاقير الطبية. هذا يشير إلى أن هذا المستقبل يمتلك يجند الوصول إليها بسهولة جيب كبير ملزم. للسماح للتحقق من إمكانية الوصول وحجم الجيب ملزم يجند. حمض ميفيناميك (2- (3,2-dimethylphenyl) حمض أمينو) وديكلورفيناك (2- (6,2-dichloranilino) حمض فينيل الخل) تم تحديدها على أنها محفزات TAS2R14 جديدة في الأونة الأخيرة في فحص سيليكون ومنبهات وأكد المقاييس الفنية وتمثل كل من المواد غير الستيرويدية المضادة للالتهابات ومتشابهة هيكلية لحمض الفلوفيناميك، والتي سبق تحديدها TAS2R14 ناهض. الجاوي (2-هيدروكسي-1،2-دي (فينيل) ethanone)، الذي يمثل أبسط العطرية كيتون الهيدروكسيل وهو عنصر طبيعي في زيت اللوز المر، وأيضا ينتمي إلى مجموعة من منبهات TAS2R14 وما شابه ذلك تقاسم وجود اثنين من فينيل نظم حلقة مع حمض الميفيناميك وديكلورفيناك. وقد لوحظت الاتصالات سيئة بين الهيدروجين من المجموعات alkoxy يجند والعمود الفقري Ile2627.35 والمشتقات ديكلورفيناك لا يمكن استيعابها في جيب ملزم بسبب عائق الفراغية. الاحتفاظ الناتجة الميفيناميك حمض البنزويل استر خصائص ناهض، على الرغم من عدم وجود تنشيط مستقبلات أقل تركيز من 10 ميكرومتر يشير إلى تقليل فاعلية، بالنسبة لكل من المشتقات الجاوي لاحظنا ردود مستقبلات قوية بالفعل بتركيزات تصل إلى 10 ميكرومتر، في حين أن التركيز الضروري من الجاوي معدلة المطلوب لتفعيل و10 ~ TAS2R14 أضعاف أعلى.



عمادة الدراسات العليا

جامعة القدس

تصنيع وتفعيل طعم المر لمستقبلات 14 (TAS2R14) -

نهج لتعيين موقعها النشط

اعداد

حذيفة رشدي كتانه

رسالة ماجستير

فلسطين - القدس

هـ-1438 / م 2017

تصنيع وتفعيل طعم المر لمستقبلات 14 (TAS2R14) -

نهج لتعيين مواقعها النشط

اعداد

حذيفة رشدي كتانه

بكالوريوس صيدلة- جامعة القدس، فلسطين.

المشرف الرئيسي: بروفيسور رفيق قرمان

قدمت هذه الأطروحة استكمالاً لمتطلبات درجة الماجستير في
التكنولوجيا الصناعية الدوائية من كلية الدراسات العليا جامعة
القدس-فلسطين.

هـ 1438 / م 2017